FORSCHUNGSZENTRUM JÜLICH GmbH

Institut für Chemie und Dynamik der Geosphäre 3: Atmosphärische Chemie

A Supplement for the RADM2 Chemical Mechanism: The Photooxidation of Isoprene

J. Zimmermann D. Poppe

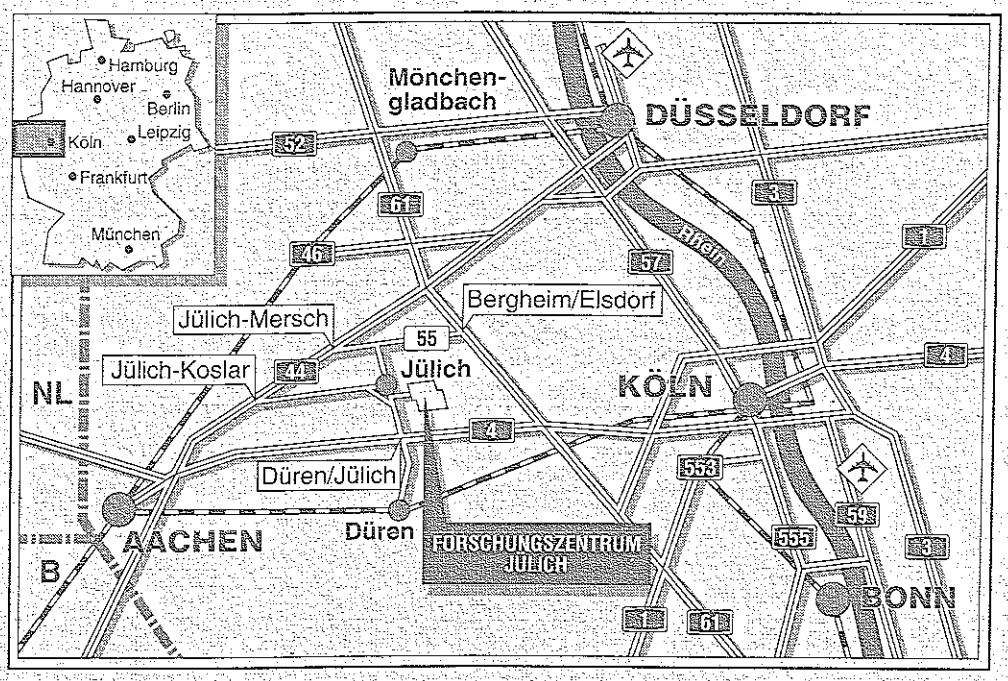

Berichte des Forschungszentrums Jülich ; 2938
ISSN 0944-2952
Institut für Chemie und Dynamik der Geosphäre 3:
Atmosphärische Chemie Jül-2938

Zu beziehen durch: Forschungszentrum Jülich GmbH · Zentralbibliothek
D-52425 Jülich · Bundesrepublik Deutschland
Telefon: 02461/61-6102 · Telefax: 02461/61-6103 · Telex: 833556-70 kfa d

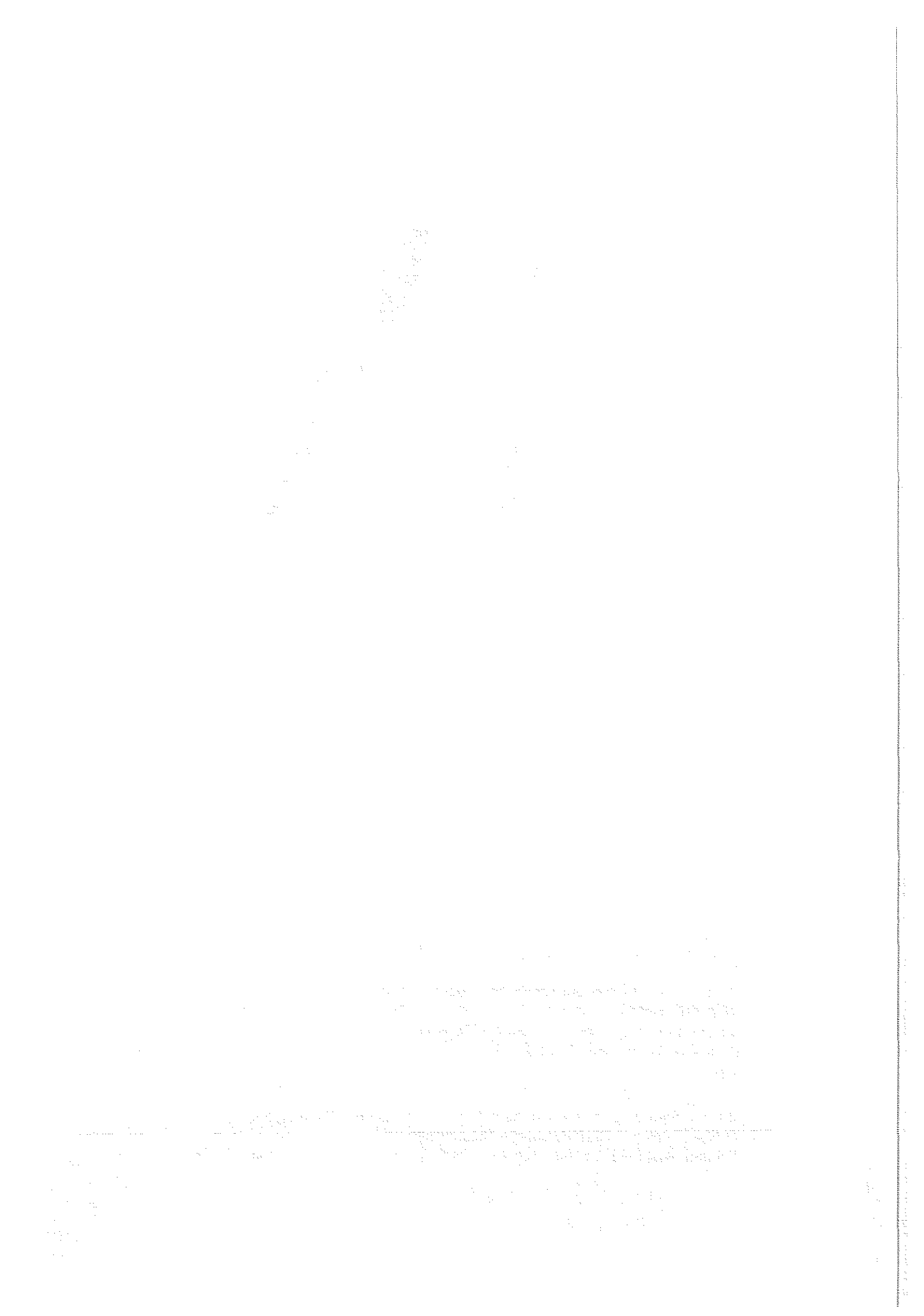

A Supplement for the RADM2 Chemical Mechanism: The Photooxidation of Isoprene

J. Zimmermann D. Poppe

Abstract

The RADM2 chemical mechanism is a scheme for the tropospheric gas phase chemistry for the use in chemistry and transport models. During recent years the importance of isoprene as a reactive biogenic hydrocarbon has been recognized. Since isoprene is poorly represented in RADM2 we have developed an extension by a comprehensive isoprene chemistry. This detailed mechanism (RADM-E) leads to the same results as RADM2 for vanishing concentration of isoprene. The main consequences are the enhanced production of organic nitrates in the course of the isoprene oxidation and the improved conservation of carbon compounds in RADM-E. The balanced C-budget brings about higher concentrations of peroxy radicals and organic peroxides. The formation of organic nitrates leads to smaller amounts of other reactive N-compounds, affecting directly NO_x, HNO_3, and PAN, and indirectly HO_x, H_2O_2, and O_3.

Since RADM-E includes 34 new species and 112 additional reactions it is not suitable for use in three dimensional transport and chemistry calculation. Therefore a condensed version (RADM-C) was developed with only 8 new species and 19 additional reactions. RADM-C gives approximately the same results as RADM-E, if $[NO_x] > 0.1$ ppb. RADM-E is also compared with the chemical mechanism of Lurmann et al. (1986), which is widely used and includes the chemistry of isoprene in a different manner.

In four scenarios, covering typical situations with high impact of isoprene, the chemical mechanisms RADM2 and RADM-C are compared, utilizing a simple 2-box-model. Differences of concentrations can exceed 10 percent for O_3 and a factor of 2 for HO_x, peroxides, NO_x, PAN, and HNO_3. Carbonyl compounds show even higher differences.

Contents

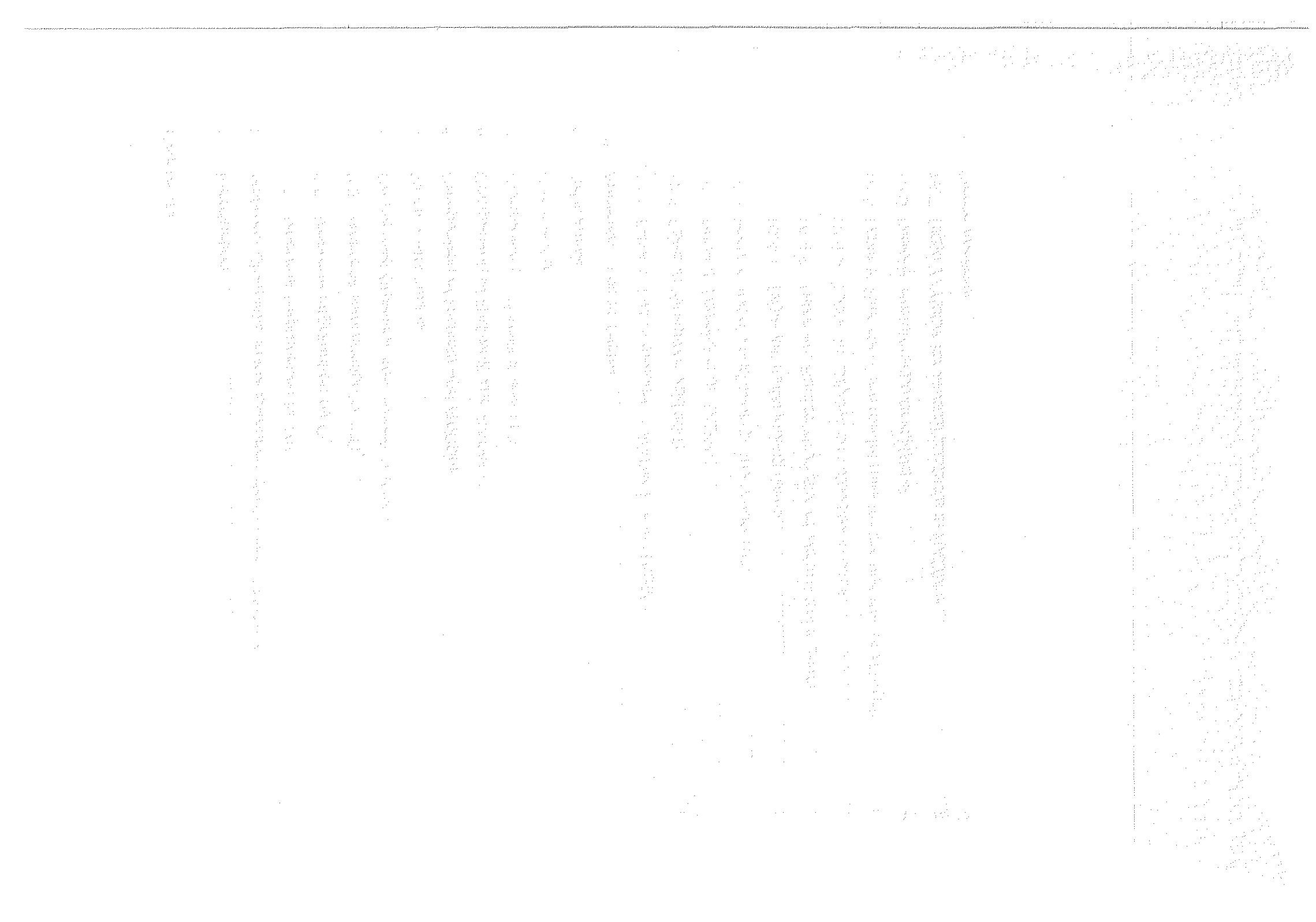

1 Introduction

The gas phase chemical mechanism is one of the most important parts of any chemistry and transport model of the atmosphere. Reliable chemical transformation rates are necessary for the correct description of the temporal and spatial distribution of emitted species and their chemical degradation products.

The Regional Acid Deposition Model is a chemical and transport scheme for the troposphere designed to model episodic events on a time scale up to several days (Chang et al., 1987). Its chemical part was designed by Stockwell (1986). This early version is denoted by RADM1 and does not contain isoprene chemistry at all. Stockwell et al. (1990) updated the scheme and introduced a very crude chemistry of isoprene. Both mechanisms have been tested against smog chamber experiments (Carter and Lurmann, 1989) and have also been intercompared with other current gas phase reaction mechanisms (Derwent, 1990, Hough, 1988, Dodge, 1989). RADM2 is also incorporated in the European Acid Deposition Model EURAD (Ebel et al., 1991). Moreover it has been used for the validation of the most important parts of the gas phase chemistry, namely the fast photochemistry. Poppe et al. (1992 and 1994) compared field data for the hydroxyl radical with model calculations using the chemical mechanism RADM2 (Stockwell et al., 1990). Reasonable agreement between model and experiment indicate that all parts of the chemistry that influence the HO concentrations are consistently described by the model. Since HO reacts with most tropospheric trace compounds, and since it is involved in the production of all photooxidants (Ehhalt, 1987), this means a validation of major parts of the RADM2 chemical mechanism. The degree of validation for specific reactions depends of course very much on their sensitivity toward HO.

However, smog chamber results indicate that RADM1 and RADM2 fail to predict reliably the concentrations of ozone and other photooxidants in the presence of one of the most important biogenic hydrocarbons, namely isoprene (Carter and Lurmann, 1989). Indeed, the isoprene chemistry is poorly represented in RADM2. Only the first step of the oxidation chain, the reaction with HO, is correctly included. Reaction products and subsequent reactions are treated in the same manner as the degradation of propene. Specific degradation products like methacrolein (MAC) and methyl vinyl ketone (MVK) are not accounted for, although these compounds are produced in an isoprene containing atmosphere at high rates due to the rapid first

step. MVK and MAC also react with HO and thus affect the fast radical chemistry. It is quite obvious that RADM2 in its present form is not capable of dealing adequately with high levels of isoprene.

Isoprene is emitted by vegetation (Lamb et al., 1985) and can build up substantial concentrations in the mixing layer in rural and remote areas (Greenberg and Zimmerman, 1984, Niki et al., 1990, Martin et al., 1991). Therefore, isoprene can have a considerable impact on the concentrations of ozone, aldehydes, peroxides, and organic acids (Trainer et al., 1987, Trainer et al., 1991, McKeen et al., 1991). For example the presence of isoprene in concentrations of one ppb could increase the ozone level up to 20 ppb. During summer many parts of Europe which are covered by forests are expected to have also significant burdens of isoprene. Thus, there is a very practical need for the EURAD model to extend its chemical part RADM2 by including an improved chemistry of isoprene. Recent publications (Tuazon and Atkinson, 1989, 1990a, 1990b, Paulson et al., 1992a, 1992b) have shed some light on the reactions of isoprene and its products. This enables us to extend the RADM2 chemical mechanism by incorporating a comprehensive isoprene chemistry. Altogether 34 new species and 112 additional reactions were introduced to treat the isoprene degradation in an explicit manner. The resulting detailed mechanism denoted by RADM-E is identical with RADM2 for vanishing isoprene. In a second step RADM-E is condensed to meet requirements as tractability and minimizing of computer costs. Eight additional species (methacrolein, methyl vinyl ketone, hydroxy acetone, glycol aldehyde, and four peroxy radicals) and 19 new reactions remain in the condensed mechanism (RADM-C). They are a minimum set of species and reactions which are essential for a satisfactory description of the isoprene degradation with respect to oxidant and organic nitrate formation. The condensation is based upon extensive sensitivity studies with RADM-E and RADM-C investigating four typical scenarios that cover many realistic situations in the planetary boundary layer (PBL). The calculations were done with a simple time dependent two-box-model for the PBL (Sillman et al., 1990) which accounts for vertical exchange due to the rise of the height of the mixed layer during the day. Such simple approach is sufficient since most of the reactive isoprene is depleted in the PBL.

During the final work for RADM-C Paulson and Seinfeld (1992) published a photooxidation mechanism for isoprene based on their kinetic results. Since we used that very same data, the isoprene part of their scheme is similar to our extensions of RADM2. Differences arise mainly from the fact that we had to be compatible with the lumping scheme of RADM2. Also we adopted slightly different chemical pathways.

We assumed that the terminal carbon atoms of isoprene are attacked by HO in 70% of all cases as indicated by the observations instead of 60% as proposed by Paulson and Seinfeld (1992). Also we included the radical yields observed by Paulson et al. (1992b) for the reaction of isoprene with ozone, while Paulson and Seinfeld used smaller yields. We neglected the photolysis of methacrolein and methyl vinyl ketone. The treatment of the carbonyl compounds was different. In addition to methacrolein, methyl vinyl ketone, and 3-methyl furane, Paulson and Seinfeld proposed the formation of eight carbonyls, which they lumped into the surrogat IALD1. We introduced only two additional compounds 4-hydroxy-2-methyl-2-butenal (HM1) and 4-hydroxy-3-methyl-2-butenal (HM2). The product speciation of degradation of 2-propenyl, which is produced during the oxidation of methacrolein, is different. Paulson and Seinfeld lumped the product into IALD1, while in our mechanism HCHO and CH_3CO is produced obeying thereby C-atom conservation. Both isoprene mechanisms are consistent with the available kinetic data, the differences show the actual uncertainty in the knowledge of the isoprene chemistry.

2 Isoprene Chemistry in the Extended Mechanism (RADM-E)

All additional reactions are compiled in table 2. Surrogates and abbreviations for substances in RADM-E are explained in tab. 1 (see also Stockwell et al., 1990). The reactions are numbered according to tables 2, a-d in Stockwell et al. (1990). Here, the photolytic reactions are denoted by "P", followed by the number in tab.2a in Stockwell et al. (1990), and the Arrhenius-type reactions are marked by "T". The new reaction equations discussed in RADM-E are numbered starting with P22 and T125, respectively.

Where stoichiometric factors are adapted from the literature, they are truncated to the significant digits and corrected within their reported errors to achieve mass balance. For example Tuazon and Atkinson (1990a) report, that the degradation of methacrolein (MAC) gives methyl glyoxal (MGLY), hydroxy acetone (HKET), peroxymethacrylic nitric anhydride (MPAN) and CO_2. The yields are 0.41±0.03 for HKET, 0.084±0.016 for MGLY and 0.50±0.16 for the sum of MPAN and CO_2. Under the assumption that these products represent all reaction pathways, in RADM-E the model stoichiometric factors are set to 0.4, 0.1, and 0.5, respectively.

RADM-E is identical with RADM2, if the isoprene concentration is zero. Only the reactions of isoprene with HO (T40), O_3 (T72), and NO_3 (T68) are changed. With

these exceptions RADM2 is converted to RADM-E by solely appending a set of new reactions and adding new substances or surrogates. Abbreviations and the definitions of surrogates of RADM2 are taken without change.

2.1 Isoprene Degradation by HO

In the troposphere isoprene reacts mainly with HO, in polluted air also in significant amounts with ozone and NO_3. For $[HO] = 10^6 cm^{-3}$, $[O_3] = 40$ ppb, and $[NO_3] = 10^7 cm^{-3}$ the lifetimes of isoprene are 2.75 h, 20 h (Atkinson, 1990), and 35 h (Wille et al., 1991), respectively. Therefore the main emphasis is on the comprehensive description of the oxidation by HO.

The addition of HO to one of the double bonds of isoprene (T40) and the consecutive reaction of the formed radical with O_2 leads to one of six peroxy radicals (denoted by ISPi, i=1...6) (see tab. 1 and 2). Although these radicals have not been measured directly, the branching between the radicals can be infered from the yields of longer lived products formed by the reactions of these peroxy radicals with NO (T131-136). These longer lived products are methyl vinyl ketone (MVK), methacrolein (MAC), and 3-methyl furane (MFUR) and they are specific for the degradation of isoprene. They were measured by Tuazon and Atkinson, (1990b) and Paulson et al.(1992a). Here the branching as reported by Paulson et al. (1992a) is adopted. The fraction yielding organic nitrates was also determined, although the chemical identification was not done in detail (Tuazon and Atkinson, 1990b). Further products are carbonyl compounds, which are not yet identified. However, for structural reasons these carbonyls are most likely 4-hydroxy-2-methyl-2-butenal (HM1) and 4-hydroxy-3-methyl-2-butenal (HM2). Paulson and Seinfeld (1992) discussed yields and chemical structures of these carbonyls in more detail. They proposed the formation of eight compounds, mostly via isomerisation reactions. Three of these compounds are cis- or trans-isomeres of HM1 and HM2, and a hydroxylated isomere of HM2. The other four compounds are two hydroxylated isomere of MAC and a mono- and a bis-hydroxylated isomeres of MVK. Their formation is accompanied by HCHO production. However, there is no experimental evidence for the existence of these intermediates and their possible subsequent degradation. We believe, that the positive correlation between the measured yields of HCHO and the observed yields of MAC and MVK indicates that carbonyls with four C-atoms do not contribute significantly to the unidentified carbonyl compounds. Therefore we should be able to describe the dominant features of these yet unknown

species by HM1 and HM2. d Moreover their reactions are unknown. Since our calculations indicated that formation of photooxidants are not sensitive to the details of the chemistry of these carbonyls, our simplified treatment adequately describes the impact on O_3, NO_x, HNO_3, PAN, peroxides and HO.

The rate constant for the reaction of isoprene with HO (T40) is adopted from RADM2. Also the rate constants for the reactions of the additional organic peroxy radicals with NO and HO_2 are taken from the corresponding reactions in RADM2. The products of the reactions of all biogenic peroxy radicals with HO_2 are lumped into the RADM2 substance OP2, which includes all organic hydroperoxides with the exception of methyl hydroperoxide. If the biogenic peroxy radicals constitute a large fraction of the total concentration of peroxy radicals, the spectrum of products and the reactivity of the surrogate OP2 should be changed accordingly. This is not done here, because the gas phase reactions of the peroxides are rather slow, their sink in the atmosphere is heterogeneous loss. The possible influence of an altered composition of OP2 on the gas phase chemistry is therefore only minor.

Under rural and polluted conditions, i.e. NO_x mixing ratios well above 0.1 ppb, the reactions with NO and HO_2 dominate the degradation of the peroxy radical ISPi (Stockwell et al., 1990). In remote areas, however, reactions among the peroxy radicals (permutation reactions) may have comparable reaction rates. Thus, 43 permutation reactions are part of the extended mechanism. Rate constants and product distributions are estimated along the lines suggested by Madronich and Calvert (1990). In addition permutation reactions of the ISPi with the methyl peroxy radical are taken into account. The self-reactions of the secondary and tertiary peroxy radicals are neglected, because they are slower by orders of magnitude compared to the reactions with primary peroxy radicals. The self-reactions of biogenic peroxy radicals formed by the oxidation products of isoprene are neglected. Because of the low reactivity of their precursors, their concentrations are small compared to the ISPi concentrations.

The relatively stable compounds MAC, MVK, MFUR, HM1, and HM2 are implemented explicitly in RADM-E. The organic nitrates are lumped into the RADM2 surrogate ONIT leading to the same problems as indicated for OP2.

The oxidation of MAC and MVK by HO was recently investigated (Tuazon and Atkinson, 1989, 1990a). In the case of MAC H-abstraction was observed which leads to a methacrylic peroxy radical (MA2P) after O_2 addition. HO-addition to a double bond is also possible. The kinetic data indicate that both paths contribute roughly equal amounts. The rate constants are taken from Atkinson (1990). The reactions of MA2P with NO (T138) and NO_2 (T152) are derived in analogy to the acetyl peroxy

radical (ACO3). The addition of NO_2 yields peroxymethacrylic nitric anhydride (MPAN) which decomposes thermally with the same frequency as PAN (Roberts and Bertram, 1992). The products of reaction T138 are taken from the reaction sequence (Tuazon and Atkinson, 1990a):

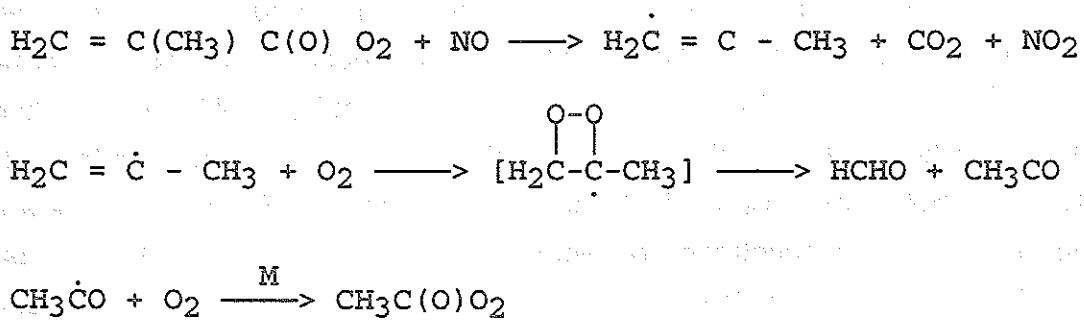

which is suggested by the analogy with the reaction of the vinyl radical with oxygen observed by Slagle et al. (1984). If only the reactions of isoprene and its products with HO and NO are considered, the proposed reaction sequence enhances the formation of HCHO by 0.28 (to a total of 2.07) and of ACO3 (and therefore PAN) by 0.14 (to a total of 0.65) per isoprene molecule destroyed. Tuazon and Atkinson (1990a) discussed this reaction sequence as plausible, they suspected however, that the observed yields of CO_2 and HCHO were not consistent with the formation of ACO3 with yields as high as 0.5 per molecule MAC. At present no improved mechanism can be suggested so that the scheme above is adopted. Paulson and Seinfeld (1992) assumed that 2-propenyl degradation contributes to their surrogate IALD1, which lumps carbonyls with four and five C-atoms. Obviously this is not a better solution, since it violates the conservation of C-atoms.

MVK reacts with HO mainly by addition at the double bond (Tuazon and Atkinson, 1989). Consequently, the H-abstraction is neglected. The rate constant is taken from Atkinson (1990). The product yields of the reactions of the associated peroxy radicals (lumped into MVKP) with NO (T139) are 0.7 for glycol aldehyde (HALD), and ACO3 and 0.3 for methyl glyoxal (MGLY), HCHO, and HO_2. MVKP is assumed to react with other organic peroxy radicals as if it is entirely the primary peroxy radical. However, its reactivity is half that of a primary peroxy radical to account for the low reactivity of the secondary peroxy radical, which is lumped into MVKP.

The rate constant for the reaction of MFUR with HO (T225) is taken from Atkinson et al. (1989a). Since MFUR contributes to the isoprene oxidation products

by only about 6 percent, a very approximate reaction scheme is sufficient in this case. A plausible degradation sequence is:

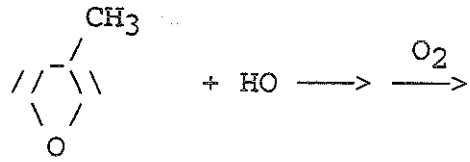

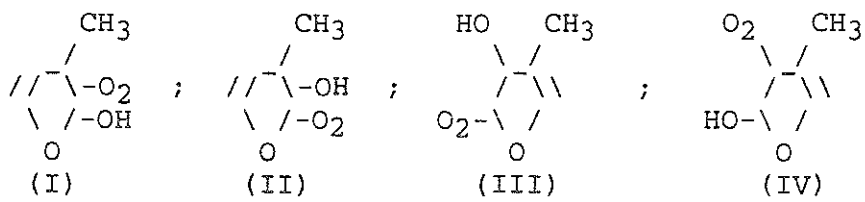

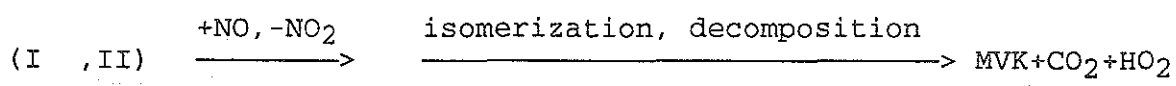

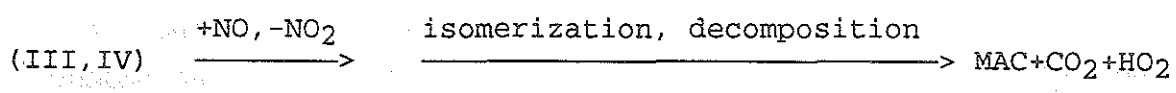

The compounds (I-IV) are lumped with equal weights into the peroxy radical surrogate MFUP, which reacts with NO as stated above to MVK or MAC (T144) and with HO_2 to OP2 (T170).

Little is known about the reactions of HMi (i = 1...2). The internal double bond is likely to be the most reactive site for HO and O_3 attack. However, H-abstraction from the carbonyl group can not be neglected. A rate constant of $4 \cdot 10^{-11} cm^3 s^{-1}$ is estimated for the reaction with HO (Atkinson, 1987) (T215, T216), leading to 0.6 HMiP (peroxy radicals from the O_2-attachment of the HO-addition products) and 0.4 HiO3 (acyl peroxy radicals produced after H-abstraction). The reactions of the HMiP with NO, which finally yield hydroxy acetone (HKET) and glyoxal (GLY), or glycol aldehyde (HALD) and methyl glyoxal (MGLY) (T142, T143), are taken in analogy to the decompositions of other alkenes. The HiO3 form PAN-like substances HPNi with NO_2 (T228, T229) and decompose in reaction with NO (T232, T233). The decomposition is similar to that of MA2P and yields HALD and ACO3 in the case of H1O3 and HKET, CO and HO_2 in the case of H2O3.

HALD is a product not only of the oxidation of HM1, but also of degradation of MVK. Here it is assumed that it reacts similar to acetaldehyde. Abstraction of the aldehydic hydrogen by HO and subsequent addition of O_2 yields an acylperoxy radical (HALP) (T127). Niki et al. (1987) report that 20 percent of the oxidation of HALD proceed by H-abstraction from the other C-atom and subsequent formation of HO_2 and GLY. Since HALD would be a minor source of both this reaction path is neglected. Alternatively HALD is photolyzed (P22). Its products decompose into HO_2, CO and HCHO:

$$HOCH_2CHO \xrightarrow{h\nu} HOCH_2 + CHO \qquad (P22a)$$

$$HOCH_2 + O_2 \longrightarrow HO_2 + HCHO \qquad (P22b)$$

$$CHO + O_2 \longrightarrow HO_2 + CO \qquad (P22c)$$

To our knowledge no kinetic data are available for the rate constants P22a and T127, which indicate that the reactivity of HALD and of acetaldehyde are different. Therefore we adopted the photolysis frequency (P22a) and the rate constant for the reaction with HO (T127) from the corresponding reactions of acetaldehyde. Reactions P22b and P22c are assumed to be very fast (Atkinson, 1990). HALP is treated similar to ACO3. Hydroxy peroxyacetic nitric anhydride (IPAN) is formed with NO_2 (T150). The reaction of HALP with NO yields an oxy radical which reacts with O_2 to HCHO, CO_2, and HO_2 (Lurmann et al., 1986) (T140).

The oxidation of ethene (OL2) (Niki et al. (1981)) forms also HALD:

$$CH_2{=}CH_2 + HO \xrightarrow{O_2} HOCH_2CH_2O_2$$

$$HOCH_2CH_2O_2 + NO \xrightarrow{O_2} 1.6\ HCHO + 0.2\ HOCH_2CHO + NO_2 + HO_2$$

Stockwell et al. (1990) have lumped HALD into ALD. So in RADM2 the reaction sequence is:

$$OL2 + HO \longrightarrow OL2P \qquad (T23)$$

$$OL2P + NO \longrightarrow 1.6\ HCHO + 0.2\ ALD + NO_2 + HO_2 \qquad (T49)$$

In RADM-E (and also RADM-C) HALD is not lumped into ALD. For consistency reasons, HALD should be treated as a product of the reaction of NO with OL2P instead of ALD with the disadvantage, that RADM-E is no longer identical with RADM2 for vanishing isoprene. In the scenarios chosen here, the replacement of ALD by HALD in reaction T49 makes no significant difference. It would, however, if OL2 is the dominant hydrocarbon. For example, due to this inconsistent lumping the concentrations of HALD and GLY are underpredicted by more than 10 percent, if the concentration of ethene (OL2) exceeds that of isoprene by more than a factor of 3. ALD and PAN are less sensitive. The overprediction for both compounds is about 10 percent if the concentration of ethene is about 20 percent of the NMHC burden. The concentrations of HO_x, NO_x, O_3, and peroxides are nearly unaltered. For reasons of simplicity and comparability it is not recommended to replace ALD by HALD in reaction T49. However, one should keep in mind, that RADM-E and RADM-C are inconsistent with respect to HALD.

HKET is produced by the oxidation of MAC and HM2. It is expected to be a measurable chemical indicator for isoprene degradation. The lifetime with respect to depletion by HO (Tuazon and Atkinson, 1990b) is t = 3.9 d for [HO] = $10^6 cm^{-3}$). The rate constant for the reaction with HO ($k = 3 \cdot 10^{-12} cm^3 s^{-1}$) is taken from Atkinson et al. (1989b). Abstraction of an H-atom and addition of O_2 leads to two peroxyradicals:

(I) (II)

We assume that (I) reacts with NO forming an organic acid lumped into ORA2 and HO_2 and that (II) decomposes to HCHO and HALP after reaction with NO. Both peroxy radicals are lumped into HKET with equal weights. The abstraction of the H-atom from the hydroxyl group is neglected.

The photolytic decomposition of MVK and MAC is neglected, since the quantum yields are very low. The products (CO_2, CO, ethene, propene, HCHO, and organic acids) are rather stable (Raber et al., 1990) and have other sources that are much larger. Paulson and Seinfeld (1992) included the photolysis of MVK and MAC, they suggested, however, very small frequencies. The influence is likely to be negligible.

2.2 Isoprene degradation by O_3

The products of the ozonolysis of isoprene are taken from Paulson et al. (1992b). The short-lived Criegee biradicals are not treated explicitedly in RADM-E. We assume that they react exclusively with H_2O following Stockwell et al. (1990). The ozonolysis of MAC (T129), MVK (T130), HM1 (T217), and HM2 (T218) is treated in analogy to that of isoprene. Values for the rate constants are taken form the upper bounds as estimated by Lurmann et al. (1986). No rate constants were reported for the reactions of HMi with ozone. Thus we estimate a common value for both reactions of $k = 5 \cdot 10^{-16} cm^3 s^{-1}$ at room temperature with an Arrhenius temperature dependence of E/R = 900 K. Both values are within the ranges reported for other alkenes (see e.g. Atkinson, 1990).

2.3 Isoprene degradation by NO_3

The rate constant for the reaction of isoprene with NO_3 is adopted from Wille et al. (1991). The products should be similar to those of the oxidation by HO. They are lumped into a nitrate (ISON), which reacts with NO, giving equal amounts of MVK and MAC, and with HO_2, forming a more stable organic nitrate, which is lumped into ONIT. The rate constants for the reactions of MAC and MVK with NO_3 are estimates by Lurmann et al. (1986). The products are treated in analogy to those of the reaction with HO. The rate constants of the reactions of the HMi with NO_3 are the same as for OLI. The further reaction sequences follow those of other alkenes in the RADM2 mechanism. The rate constants for the reactions of HALD and HKET with NO_3 are adopted from Lurmann et al. (1986).

3 Condensed Chemical Mechanism RADM-C

The condensed mechanism (see tab. 3) is designed to fulfill two conditions. First, it should include explicitly only those products of the isoprene degradation, for which a comparison with field experiments is possible or seems to be feasible in the near future. Thus, it contains MVK and MAC, which can be measured and which are important and specific degradation products of isoprene (see for example Martin et al., 1991). HKET is also included as a specific degradation product of isoprene. It is

potentially important for the validation of the atmospheric isoprene chemistry if measurements become feasible (Tuazon and Atkinson, 1990b). Second, it should give correct yields of at least O_3, NO_x, HO, peroxides, aldehydes, and PAN. Sensitivity studies showed, that the inclusion of HKET and HALD is essential for correct predictions of the concentrations of HCHO, higher aldehydes (ALD), PAN, and peroxides. These four carbonyls (MAC, MVK, HALD, and HKET) are included together with the associated peroxy radicals. These are a peroxy radical (ISOP) from the isoprene-HO reaction and two (MVKP, MACP) for the reactions of MAC and MVK with HO and an isoprene-NO_3-adduct (ISON). A further peroxy radical (MA2P) is not accounted for, since its reaction with NO_2 has only small rates leading to MPAN mixing ratios in the sub-ppb-range even at high isoprene concentrations.

Some short-lived substances (MFUR, HM1, HM2, HALP, HKEP, MA2P, MACN, and MVKN) are included but they are not treated explicitly. They are assumed to be in quasi steady state. Additional losses to compounds not included in RADM-E are not taken into account, for example from reactions with HO_2 and other peroxy radicals. Sufficiently accurate yields are to be expected for NO_x mixing ratios larger than 0.1 ppb. Two products of the reaction of ISOP with NO and the selfreaction of ISOP react to a considerable percentage with ozone thereby producing HO. The ozonolysis of the HMi is taken into account in the production yields of the reactions of ISOP leading to HO production in the reaction with NO and in its selfreaction. Some compounds (DOC, MPAN, IPAN, DPAN) are neglected, which contribute little to the overall reactivity of the mechanism, i.e. with typical reaction rates < $10^3 cm^{-3} s^{-1}$.

4 Model Calculations

The three mechanisms (RADM2, RADM-E, and RADM-C) were compared in calculations with a simple one-dimensional (2-box) model which incorporates fast vertical transport within the planetary boundary layer (PBL) and an exchange with the free atmosphere as described by Sillman et al. (1990). The runs do not intend to model a specific episod, instead initial conditions and emissions are chosen to demonstrate the different impact of isoprene within the three mechanisms.

The parameterization of the diurnal cycles of the height of the PBL, temperature, and sources of NO_x and isoprene are rather crude. The scenarios share the same diurnal cycle of the height h(t) of the PBL. The mixing height is 100 m from 21.00 to 7.00°LT. Then h(t) increases with 26% h^{-1} till 17.00°LT when the

maximum height of 1000 m is reached. From 17.00 to 18.00 LT it drops rapidly to 139 m, and from 18.00 to 21.00 LT it decreases to 100 m. The frequency of exchange with the free troposphere is $10^{-5}s^{-1}$.

The temperature is 293 K from 21.00 to 7.00 LT and varies linearly to a maximum of 308 K at 16.00 LT. Thereafter it drops linearly to its nighttime value. The isoprene flux Q is a function of the temperature T and incident photosynthetic active radiation (Lamb et al., 1985) Here the latter is be parameterized by the photolysis frequency of ozone, $J(O_3)$, yielding O^1D :

$$Q = f(T) \cdot g(J) \qquad (1)$$

where f(T) models the exponential dependence on T

$$f(T) = Q_1 (Q_2/Q_1)^{\xi} \qquad (2)$$

with

$$\xi = \frac{T - T_1}{T_2 - T_1} \qquad (3)$$

The parameters Q_i are measured maximum values for a deciduous forest (Lamb et al., 1985) with $Q_1 = 10^{10} cm^{-2}s^{-1}$ and $Q_2 = 2 \cdot 10^{12} cm^{-2}s^{-1}$ for $T_1 = 273$ K and $T_2 = 303$ K, resp. The influence of the radiation is modeled by

$$g(J) = J(O_3) \; / \; J_{max}(O_3) . \qquad (4)$$

where J_{max} is the maximum J-value at noon. The diurnal cycle of Q adopting these experimental data is displayed in figure 1.

Explorative calculations indicated that the results of a comparison between RADM2, RADM-E, and RADM-C are mainly determined by the NO_x level. Temperature and radiation are less important, since the first and usually rate determining step, the reaction of HO with isoprene is the same in all mechanisms. Therefore, the scenarios are characterized by different levels of $[NO_x]$ and appropriate concentrations of the hydrocarbons covering thereby conditions of clean to polluted air.

All calculations are for summer solstice. In table 4 the initial conditions of the calculations for the scenarios are summarized. Scenario 1 investigates remote tropical conditions (23° N) with clean air (NO_x emission rate at $2 \cdot 10^9 cm^{-2}s^{-1}$), high humidity ($H_2O$ mixing ratio 3 percent), and high radiation. Scenario 2 simulates a

rural situation at 50°N with a NO_x emission rate of $2 \cdot 10^{10} cm^{-2} s^{-1}$. A suburban situation is modelled in scenario 3 with a NO_x-emission strength that varies with time. Scenario 4 discusses an urban situation with a large NO_x emission rate of $10^{12} cm^{-2} s^{-1}$. Details of the treatment of CO and the hydrocarbons are somewhat different for the scenario. They are specified in table 4b. The calculations simulate an episode of 84 hours starting at local noon. After a transition period of about 60 hours many compounds, in particular the photooxidants, approach nearly periodic diurnal cycles in the lower box. The comparison between the different mechanisms refer to the results of the last day of the simulation.

5 Comparison of RADM2 and RADM-E

The most decisive difference between RADM2 and RADM-E is already given by the different product spectrum of the initiating reaction of isoprene with HO :

(1) In RADM2 the products of the oxidation of isoprene are the same as for the oxidation of propene implying that the higher carbonyls produced by the oxidation of isoprene are lumped into ALD, which is given the same reactivity as acetaldehyde. In RADM-E these carbonyls are treated separately from ALD by MAC, MVK, HM1, and HM2. These carbonyls have entirely different reactivities and product spectra compared to ALD. Although the definition and therefore the properties of ALD are the same in RADM2 and RADM-E, the RADM2-surrogate ALD represents biogenic carbonyls, too. To distinguish between them in the discussion below, ALD of RADM2 and RADM-E is denoted by ALD_2 and ALD_e, respectively. As long as there is no isoprene, ALD_2 and ALD_e are identical. In the presence of isoprene, ALD_2 also encompasses biogenic carbonyls not included in ALD_e.

(2) In contrast to RADM2 the oxidation of isoprene in RADM-E leads to the production of organic nitrate lumped into ONIT (Stockwell et al., 1990) . The reactions of the ISPi with NO yield 12 percent ONIT, which can be a significant source of ONIT. Relative to RADM2 there is a redistribution of nitrogen compounds in favor of long lived organic nitrates. Especially, concentrations of NO_x, HNO_3, and PAN are lower in RADM-E than in RADM2.

(3) Due to the improved chemistry the carbon is nearly conserved during the isoprene degradation. The formation of ONIT and OP2 and some of the peroxy

radical permutation reactions violate carbon conservation, however, the carbon loss is negligibly small.

All differences are expected to be particularly effective under low NO_x-conditions. Here we discuss the results (fig. 2a-g) for the NO_x-poor rural scenario for mid latitudes (scenario 2) first. Compared to RADM2 the production of the organic nitrates (ONIT) is higher by a factor of 3 at noon and up to 8 in the evening which reduces [NO_x] by about a factor of 5 to 8 in the afternoon (fig. 2a, b). During this time the lower NO concentration weakens the recycling of HO and HO_2 so severely that HO in RADM-E vanishes practically an hour earlier than in RADM2. Consequently 50 percent less HNO_3 is produced. The precursors of PAN, NO_2 and ACO3, behave differently in RADM2 and RADM-E. The nitrogen dioxide level is lower in RADM-E and the concentration of ACO3 is enhanced. The main effect is an advance of the peak concentration of PAN by about one hour in RADM-E compared to RADM2 (fig. 2c). Also the daily maximum of PAN is about 25 percent higher in RADM-E, but in the afternoon the PAN concentration in RADM2 exceeds that of RADM-E by a factor of 3. The lower NO_x concentration in RADM2 reduces slightly the production of O_3 (6 percent, or 4 ppb at the peak concentration).

The decreased HO abundance in RADM-E weakens the isoprene degradation resulting in an enhancement of the isoprene concentration by about 25 percent (fig. 2h). Lower NO_x concentration and higher nighttime abundance of isoprene in RADM-E cuts [NO_3] during the night by 50 percent.

HCHO has a lower concentration not only due to reduced [HO], but also because of the reduced yield during the improved isoprene degradation in RADM-E. OLTP, the peroxy radical associated with isoprene in RADM2, releases one HCHO molecule in the reaction with NO, whereas the reactions of NO with the peroxy radicals ISPi specific for isoprene in RADM-E yield only 0.6 molecules HCHO on the average (T131-T136).

Lower recycling of HO_2 by NO increases the HO_2 concentration in RADM-E, leading to a 36 percent higher concentration of H_2O_2 (fig. 2f). The additional organic species, which are released by the isoprene oxidation require more degradation steps in RADM-E, produce more peroxy radicals, and enhance the abundance of OP2 by more than a factor of 4 (fig. 2g).

Obviously the chemical representation of aldehydes in RADM-E is much better than in RADM2. The sum of ALD_e, MVK, HMi, and MFUR corresponds roughly to ALD_2 in RADM2. The relation is only approximately valid depending on the NO_x level, because the losses to organic nitrates are also losses of carbonyl compounds.

Moreover the reactivities of these compounds are different from the reactivity of ALD_2.

In contrast to RADM2 where GLY and MGLY are mainly products of the oxidation of aromates in RADM-E a potential source of these compounds are the destruction of carbonyls following the isoprene oxidation. Depending on the isoprene relative to the aromates concentration MGLY and GLY can build up significant concentrations. Many of the findings for scenario 2 hold also for the scenario 1 (no figure given). The NO_x-level is considerably lower which enlarges the differences between RADM2 and RADM-E. For example an even larger fraction of NO_y is stored in organic nitrates. Also the H_2O_2 mixing ratio is affected according to a different partitioning of HO_x into HO and HO_2.

The reduced recycling of HO_2 by NO is compensated by the enhanced HO_2 destruction by biogenic peroxy radicals. With exception of the morning hours, $[HO_2]$ is diminished up to more than a factor 2 in the afternoon, when biogenic peroxy radicals are present due to the isoprene oxidation. Therefore, the H_2O_2 concentration is reduced by 40 percent in RADM-E. However, [HO] is up to a factor of 2 higher in the afternoon, and more than a factor of 5 in the night, because then the ozonolysis of isoprene and of its degradation products serves as the dominant source of HO in RADM-E.

The importance of the permutation reactions of the ISPi is demonstrated in the diurnal cycle of [HCHO]. Higher concentrations and a 5 hour delay of the peak concentration in RADM-E are the result of a high production of HCHO by permutation reactions lacking completely in RADM2.

Scenario 3 for a suburban situation serves as an example for a high NO_x situation (fig. 3a-g). The concentration of ONIT in RADM2 and in RADM-E differs still by a factor of 4 (fig. 3a). The diurnal cycle of the NO_2 mixing ratio exhibits now three maxima. As in the other scenarios the maxima early in the morning and in the late afternoon are caused by the interplay between the varying height of the mixed layer and the varying photolysis of NO_2. The third peak in this scenario is caused by the substantial day time emissions of NO which is rapidly converted to NO_2 in the presence of O_3. However, $[NO_2]$ is only about 20 per cent reduced in RADM-E (fig. 3b). Since the reaction with NO_2 is now the dominant sink for HO the decrease of NO_x in this case means an increase of the concentration of OH (about 15 percent higher peak value), of O_3 (about 8 percent or 8 ppb), of HO_2 (nearly a factor of 2), of H_2O_2 (factor 3), of OP1 (factor 2), and of OP2 (factor 5). The lower recycling rate of radicals by NO enhances the concentrations of the peroxides additionally. However, [PAN] and $[HNO_3]$ are approximately the same in RADM2 and RADM-E, because the

lower NO_2 concentration is compensated by higher concentrations of ACO3 or OH on the daily average.

The differences between RADM2 and RADM-E depend strongly on the level of NO_x (see table 5). At high NO_x levels the formation of organic nitrates is limited by the isoprene abundance. In urban case, scenario 4, for example the difference for $[NO_x]$ is as low as 10 percent, thus leading to lower discrepancies for all substances. Especially $[O_3]$ differs by less than 2 percent. The main cause for decreasing differences is the reduction of the production of organic nitrates with increasing NO_x. This makes the budget of photooxidants and nitrogen oxides less sensitive to the different treatment of N-containing compounds in RADM2 and RADM-E.

6 Comparison of RADM-E and RADM-C

RADM-E and RADM-C are in much closer agreement with each other than either with RADM2. Main differences arise from the lumped reactions of the biogenic peroxy radicals and from the different reactions with NO_3.

The lower number of degradation steps reduces the total concentration of biogenic peroxy radicals in RADM-C. As a consequence the distribution of ROOH among the different peroxide species changes. Thus, the concentration of OP2 is lowered up to about 10 percent in RADM-C. Since HO_2 and MO2 have less other peroxy radicals to react with their concentrations are higher (80 percent for $[HO_2]$ in the remote case in the afternoon, 5 percent for the rural and the suburban cases). Similarly the production of peroxides is larger in RADM-E than RADM-C, for example of H_2O_2 (35 percent in the remote case, less than 10 in other cases), and of OP1 (12 percent in the remote case, less in other cases).

The nighttime chemistry in RADM-E and RADM-C differ considerably, if NO_3 concentrations are large, for example in the presence of high O_3 and NO_2 mixing ratios. Then the reactions of NO_3 with the biogenic compounds become important. The severest simplification in the NO_3-chemistry of RADM-C is, that NO_3-reactions of MAC and MVK do not produce the reactive organic nitrates MACN and MVKN. Instead the surrogat OLN is formed, which contains also the nitrates formed by alkenes. The reaction of OLN with NO yields HCHO and ALD, whereas the reactions of MACN and MVKN with NO produce HCHO and MGLY. In RADM-E about 70 percent of MGLY are produced by the reaction of MVKN with NO in the suburban case at night. Due to the neglection of this nighttime source for MGLY in RADM-C

the concentration of MGLY is lower by about 40 percent. Moreover, in the suburban case 50 percent of HALD are depleted by NO_3 during the night in RADM-E. Since this reaction is not part of RADM-C, the condensed mechanism predicts higher HALD concentrations up to 25 percent. In both cases these errors due to the condensation do not affect the day time concentrations, and have no influence on the concentrations of other stable substances.

The degree of performance of RADM-C is expressed by the relative mean deviation σ (equation 5) and the relative mean bias b (equation 6). They are calculated for some key substances (NO_2, O_3, H_2O_2, HO, HO_2, HCHO, and PAN). The means are taken over the hourly calculated concentrations of the last day (n = 24) of each scenario, where i denotes the hour and the indices e and c denote RADM-E and RADM-C:

$$\sigma = \frac{\sqrt{\frac{\sum\left(c_{e,i} - c_{c,i}\right)^2}{n}}}{\frac{\sum c_{e,i}}{n}} \qquad (5)$$

$$b = \frac{\frac{\sum c_{e,i} - c_{c,i}}{n}}{\sum \frac{c_{e,i}}{n}} \qquad (6)$$

The calculated values of b and σ are displayed in table 6, together with the smallest and largest relative differences between RADM2 and RADM-E.

In most cases σ is small with values below 20 per cent. PAN is an exception with higher values in scenarios 1 and 2, other exceptions are HO in scenario 2 with 44 per cent and HO_2 and H_2O_2 in scenario 1. The latter is simply a result of the higher amount of peroxy radicals in RADM-E compared to RADM-C. Since their reactions with HO_2 is the dominant sink of in scenario 1 and thereby controls H2O2 as well.

The bias is sometimes considerable, too. Especially [PAN] is higher by 61 percent in the remote case, 35 percent in the rural case and 15 percent in the suburban case in RADM-C. This is due to a higher concentration of ACO3, into which HALP and MA2P are lumped in the condensed scheme. Generally, the performance is worse in scenario 1 compared to the other scenarios, except for O_3,

HO, and HCHO. HO is also significantly higher (21 percent) in the rural case in RADM-C.

However, taking into account all scenarios, the results of RADM-C agree well with those of RADM-E. The higher biases in scenario 1 are of minor importance, since under such conditions the permutation reactions of peroxy radicals are important, whose rate constants are rather uncertain by a factor of 2 (Atkinson et al., 1989). Thus the higher biases are connected with the higher uncertainty of RADM-E.

The shapes of the diurnal cycles are similar for both schemes. Exceptions of this rule are: [HCHO] peaks about 2 hours earlier in RADM-C in scenario 2 and 1 hour earlier in scenario 3. [H_2O_2] peaks 1 hour earlier in scenario 1 and [PAN] 1 hour earlier in scenario 3.

The agreement of the concentrations of MAC, MVK, HALD, and HKET is typically within 10 percent.

7 Comparison of RADM-E and LLA

RADM-E is compared with the chemical mechanism of Lurman et al. (1986) (in the following denoted by LLA). LLA is a detailed mechanism (276 reactions, 136 substances) with lumped molecules. It is mainly an update of an elder mechanism enriched by the isoprene chemistry from Lloyd et al. (1983) which has been used as basis for many other chemical mechanisms since then (see e.g. Trainer et al. (1987) and Hough (1991)).

For the comparison the procedure of Hough (1988) is partly adopted:

1. The inorganic chemistry is replaced by that of RADM2.
2. The rate constants of all reactions of isoprene and of MVK with HO are changed to the values in RADM-E. LLA distinguishes between anthropogenically and biogenically produced methyl glyoxal, MGLY and MGGY, respectively. Both species undergo the same reactions with the exception of the photolysis of MGGY which is higher by a factor of 8 (Lloyd et al. (1983)). We have taken the photolysis frequency of RADM-E.
3. The concentrations of the hydrocarbons in LLA are chosen to give the same reactivity as those in the other mechanisms. HC3 of RADM2 is half represented by ALK4 and half by EOH (ethanol) in LLA. HC5 of RADM-E is represented by ALK7, scaled by 0.8.

Both schemes exhibit some differences with respect to the chemistry of isoprene that are summarized as follows: Since in LLA 10 percent of the peroxy radicals of isoprene, methyl vinyl ketone, and methacrolein react with NO forming organic nitrates, the loss of NO_x to NO_y due to isoprene degradation is very similar in LLA and RADM-E. But these organic nitrates are not treated in LLA as products and therefore the budget of organic nitrates and NO_y is not properly balanced. In particular these nitrates can not serve as a reservoir of NO_x in LLA.

The products of the isoprene degradation are formed with different yields in the two mechanisms. MACR (which is MAC in LLA) and MVK are produced to equal amounts. HCHO is formed in a 50 percent higher yield in the first oxidation step in LLA. GLY and HKET are not product of the oxidation of isoprene.

We begin with the comparison of LLA and RADM-E for scenario 2 without isoprene to be able to distinguish between the effects induced by isoprene chemistry and the other parts of the mechanism. In general the differences are small, however, LLA produces about 50 percent (up to 0.45 ppb) more HCHO and 50 percent (up to 0.13 ppb) more H_2O_2 then RADM2, whereas O_3 and N-containing species are approximately the same in RADM2 and LLA. We assume, that these differences are small against those caused by differences in the isoprene chemistry. In scenario 2 now including isoprene LLA and RADM-E give partly rather similar results. [NO_x] (fig. 4a) agrees within 10 percent and [O_3] within 5 percent. In LLA the diurnal cycle of [HNO_3] is similar to that in RADM-E, but advanced by one hour. [H_2O_2] is up to 20 percent higher in LLA. The peaks of [HO] and [HO_2] are one hour earlier and about 10 percent higher. In LLA [HCHO] is up to 20 percent lower during the night (fig. 4d). It peaks at 9.00 LT, 5 hours earlier than in RADM-E, with a maximum that exceeds the peak value of RADM-E by 20 percent. The concentrations of higher aldehydes are up to 60 percent higher in LLA, of PAN and higher carboxylic nitric anhydrides are up to 40 percent in the day-time and up to a factor of 2 in the night. The isoprene concentration is up to 40 percent higher at night time and less than 20 percent at day. The concentrations of MAC and MVK differ by less than 10 percent at day.

In scenario 3 the differences between both chemical mechanisms are more pronounced. This is partly due to the fact, that the concentration of HO is higher than for RADM2. In RADM-E this leads to a closer coupling of the concentrations of ONIT to that of NO_2 and to a higher production of ONIT, since isoprene is oxidized by HO to a larger fraction. Since the organic nitrates of isoprene, MAC, and MVK are not included in LLA, there is an overestimation of the loss of NO_x. So, [NO_2] is lower by 10 to 25 percent. This leads to a 5 percent or 5 ppb higher peak concentration of O_3. [HO_2] is higher by about 20 percent and [H_2O_2] by a factor of 1.5 to 2. [HNO_3] is not

significantly different in LLA and RADM-E. [HO] is much higher between 5.00 and 10.00 LT, up to a factor of 3, but about 10 percent lower between 12.00 and 16.00 LT. [HCHO] is 10 to 20 percent higher, and the concentrations of higher aldehydes are up to 25 percent lower. The concentrations of carboxylic nitric anhydrides are more than a factor of 2 lower at night and about 10 to 20 percent lower between 11.00 and 17.00 LT. Although isoprene concentrations differ by less than 20 percent, MACR is higher than MAC by nearly a factor of 2 in the afternoon. The MVK concentration is up to 20 percent higher in LLA compared to RADM-E. The concentration of HALD is up to 40 percent lower in LLA. The concentration of MPAN differs by less than 10 percent except in the first hours after sunrise, when it is up to 50 percent higher in LLA.

The question which mechanism has better performance depends on the problem to be dealt with. Since LLA has a better resolved representation of the organic emitted trace gases it does a better job on their degradation. However, RADM-E properly balances the organic nitrates and therefore the NO_x budget. Presumably it will also predict the production of photooxidants more accurately. Final answers can only be deduced from comparisons with experiments.

8 Conclusions

The differences between RADM2 and RADM-E are caused by the improved isoprene chemistry implemented in RADM-E. For vanishing isoprene abundance both schemes give identical answers. For NO_x above 2 ppb the discrepancies are only minor and affect dominantly the specific degradation products of isoprene. Below 2 ppb the extension of RADM2 to RADM-E is necessary for the ability of the chemical mechanism to predict the concentrations of peroxides, PAN, NO_x, HNO_3, and aldehydes. Since field measurements indicate that high isoprene mixing ratios under low NO_x concentrations are frequently encountered during summer in rural areas (Niki et al., 1990, Martin et al., 1991), the extension of RADM2 by an isoprene degradation mechanism is recommended.

There are two main problems in RADM2 which are removed by the improved isoprene chemistry in RADM-E. The first is the absence of one or more peroxy radicals emerging from the adduct of HO and isoprene, which can react with NO forming organic nitrates (ONIT). Consequently RADM2 underestimates the ONIT production and overestimates the concentrations of other N-compounds, e.g. NO_x,

HNO_3, and PAN. The second is, that the number of oxidation steps and therefore the yield of peroxy radicals is too small. RADM2 thereby violates the conservation of carbon. In RADM2 40 per cent of the carbon in isoprene get lost in the first oxidation step. Both problems are approximately solved in RADM-E, where the carbon is conserved to 95.2 per cent, if only the reactions with HO and NO are considered. The production of organic nitrates ONIT and organic peroxides OP2 is a loss of carbon, because both surrogates contain only three carbon atoms.

RADM-C takes a position between RADM2 and RADM-E, since about 90 per cent of the carbon are conserved during the oxidation of isoprene. With the exception of the remote case RADM-C gives within a few percent the same results as RADM-E. The use of RADM-C is recommended since it is more time-efficient and simpler than of RADM-E. The discrepancies in the range of 10 - 30 percent for peroxides and aldehydes in the remote case are small against errors from the highly uncertain rate constants of the permutation reactions of the peroxy radicals.

The comparison of RADM-E with LLA indicates that there is a real need for an updated chemical mechanism for the isoprene degradation, since the results of the two mechanisms differ substantially, especially for $[NO_x] > 1$ ppb.

Acknowledgement

The authors wish to thank Frau Helga London for their help during the final editing of the manuscript.

9 References

Atkinson R. (1987) A structure-activity relationship for the estimation of rate constants for the gas phase reactions of OH radicals with organic compounds. *Int. J. Chem. Kinet.* **19**, 799 - 828.

Atkinson R., Aschman S.M., Tuazon E.C., Arey J., Zielinska B: (1989a): Formation of 3-methylfuran from gas-phase reaction of OH radicals with isoprene and the rate constant for its reaction with the OH radical. *Int. J. Kinet.* **21**, 593 - 604.

Atkinson R. (1990) Gas-phase tropospheric chemistry of organic compounds: A review. *Atmospheric Environment* **24A**, 1 - 41.

Atkinson R., Baulch D.L., Cox R.A., Hampson R.F., Kerr J.A., and Troe J. (1989b) Evaluated kinetic and photochemical data for atmospheric chemistry: Supplement III. *J. Phys. Chem. Ref. Data* **18**, 881 - 1097.

Carter W.P.L. and Lurmann F.W. (1989) Evaluation of the RADM gas phase chemical mechanism. *EPA/600/3-90/001.*

Chang J.S., Brost R.A., Isaksen I.S.A, Madronich S., Middleton P., Stockwell W.R., and Walcek C.J. (1987) A three-dimensional eularian acid deposition model: Physical concepts and formulation. *J. Geophys. Res.* **92**, 14681 - 14700.

Derwent R.G. (1990) Evaluation of a number of chemical mechanisms for their application in models describing the formation of photochemical ozone in Europe. *Atmospheric Environment* **24A**, 2615 - 2624.

Dodge M. (1989) A comparison of three photochemical oxidant mechanisms. *J. Geophys. Res.* **94**, 5121 - 5136.

Ehhalt D.H. (1987) Free radicals in the atmosphere. *Free Radical Research Communications* **3**, 153-164.

Greenberg J.P. and Zimmerman P.R. (1984) Nonmethane hydrocarbons in remote tropical, continental, and marine atmospheres. *J. Geophys. Res.* **89**, 4767 - 4778.

Hass H., Description of the EURAD Chemistry-Transport-Model Version 2 (CTM2) in: A. Abel, F. M. Neubauer, P. Speth (eds): Mitteilungen aus dem Institut für Geophysik und Meteorologie der Universität zu Köln, Heft 83, 1991.

Hough A. (1988) An intercomparison of mechanisms for the production of photochemical oxidants. *J. Geophys. Res.* **93**, 3789 - 3812.

Hough A. (1991) Development of a two-dimensional global tropospheric model: Model chemistry. *J. Geophys. Res.* **96**, 7325 - 7362.

Lamb B., Westberg H., Allwine G., and Quarles T. (1985) Biogenic hydrocarbon emissions from deciduous and coniferous trees in the united states. *J. Geophys. Res.* **90**, 2380 - 2390.

Lloyd A.C., Atkinson R., Lurmann F.W., and Nitta B. (1983) Modeling potential ozone impacts from natural hydrocarbons, 1, Development and testing of a chemical mechanism for the NO_x-air photooxidations of isoprene and a-pinene under ambient conditions. *Atmospheric Environment* **17**, 1931 - 1950.

Lurmann F.W., Lloyd A.C., and Atkinson R. (1986) A chemical mechanism for use in long-range transport/acid deposition computer modeling. *J. Geophys. Res.* **91**, 10905 - 10936.

Madronich S. and Calvert J.G. (1990) Permutation reactions of organic peroxy radicals in the troposphere. *J. Geophys. Res.* **95**, 5697 - 5715.

Martin R.S., Westberg H., Allwine E., Ashman L., Farmer J.C., and Lamb B. (1991) Measurement of isoprene and its atmospheric oxidation products in a central Pennsylvania deciduous forest. *J. Atmos. Chem.* **13**, 1 - 32.

McKeen S.A., Hsie E.-Y., and Liu S.C. (1991) A study of the dependence of rural ozone on ozone precursors in the eastern united states. *J. Geophys. Res.* **96**, 15377 - 15394.

Niki H., Maker P.D., Savage C.M., and Breitenbach L.P. (1981) An FTIR study of mechanisms for the HO radical initiated oxidation of C_2H_4 in the presence of NO: Detection of glycolaldehyde. *Chem. Phys. Lett.* **80**, 499 - 503.

Niki H., Maker P.D., Savage C.M., and Hurley M.D. (1987) Fourier transform infrared study of the kinetics and mechanisms for the Cl-atom- and HO-radical-initiated oxidation of glycolaldehyde, *J. Phys. Chem.* **91**, 2174-2178.

Niki H. (1990) Biogenic and anthropogenic hydrocarbon concentrations at some rural sites in the eastern part of North America. In Becker, K.H. (ed.): Comission of the European Communities, Directorate-General for Science, Research and Development, Air Pollution Research Report 33, Joint Workshop COST 611/ Working Party 2 and EUROTRAC, Sept. 25 - 27, 1990, pp. 14 - 22.

Paulson S.E., Flagan R.C., and Seinfeld J.H. (1992a) Atmospheric photooxidation of isoprene. Part I: The hydroxyl radical ground state atomic oxygen reactions. *Int. J. Chem Kinet.* **24**, 79 - 101.

Paulson S.E., Flagan R.C., and Seinfeld J.H. (1992b) Atmospheric photooxidation of isoprene. Part II: The ozone-isoprene reaction. *Int. J. Chem Kinet.* **24**, 103 - 125.

Paulson S.E. and Seinfeld J.H. (1992): Development and evaluation of a photooxidation mechanism for isoprene, *J. Geophys. Res.* **97**, 20703-20715.

Poppe D., Wallasch M., Zimmermann J., Dorn H.-P., and Ehhalt D.H. (1992) Comparison of the tropospheric concentration of OH with model calculations. *Ber. Bunsenges. Phys. Chem.* **96**, 286 - 290.

Poppe D., J. Zimmermann, R. Bauer, T. Brauers, D. Brüning, J. Callies, H.-P. Dorn, A. Hofzumahaus, F.-J. Johnen, A. Khedim, H. Koch, R. Koppmann, H. London, K.-P. Müller, R. Neuroth, Ch. Plaß-Dülmer, U. Platt, F. Rohrer, E.-P. Röth, J. Rudolph, U. Schmidt, M. Wallasch, and D. H. Ehhalt: A Comparison of Measured OH concentrations with model calculations, accepted for publication in J. Geophys. Res. 1994.

Raber W., Meller R., and Moortgat G.K. (1990) Photooxidation study of some carbonyl compounds of atmospheric interest. In Becker, K.H. (ed.): Comission of the European Communities, Directorate-General for Science, Research and Development, Air Pollution Research Report 33, Joint Workshop COST 611/ Working Party 2 and EUROTRAC, Sept. 25 - 27, 1990, pp. 91 - 95.

Roberts J.M. and Bertram S.B. (1992) The thermal decomposition of peroxy acetic nitric anhydride (PAN) and Peroxymethacrylic nitric anhydride (MPAN). *Int. J. Chem. Kinet.* **24**, 297 - 307.

Sillman S., Logan J.A., and Wofsy S.C. (1990) The sensitivity of ozone to nitrogen oxides and hydrocarbons in regional ozone episodes. *J. Geophys. Res.* **95**, 1837 - 1851.

Slagle I.R., Park J.-Y., Heaven M.C., and Gutman D. (1984) Kinetics of polyatomic free radicals produced by laser photolysis. 3. Reaction of vinyl radicals with molecular oxygen. *J. Am. Chem. Soc.* **106**, 4356 - 4360.

Stockwell W.R. (1986) A homogeneous gas phase mechanism for use in a regional acid deposition model. *Atmospheric Environment* **20**, 1615 - 1632.

Stockwell W.R., Middleton P., Chang J.S., and Tang X. (1990) The second generation regional acid deposition model chemical mechanism for regional air quality modeling. *J. Geophys. Res.* **95**, 16343 - 16367.

Trainer M., Hsie E.Y., McKeen S.A., Tallamraju R., Parrish D.D., Fehsenfeld F.C., and Liu S.C. (1987) Impact of natural hydrocarbons on hydroxyl and peroxy radicals at a remote site. *J. Geophys. Res.* **92**, 11879 - 11894.

Trainer M., Buhr M.P., Curran C.M., Fehsenfeld F.C., Hsie E.Y., Liu S.C., Norton R.B., Parrish D.D., Williams E.J., Gandrud B.W., Ridley B.A., Shetter J.D., Allwine E.J., and Westberg H.H. (1991) Observations and modeling of the reactive nitrogen photochemistry at a rural site. *J. Geophys. Res.* **96**, 3045 - 3063.

Tuazon E.C. and Atkinson R. (1989) A product study of the gas-phase reaction of methyl vinyl ketone with the OH radical in the presence of NO_x. *Int. J. Chem. Kinet.* **21**, 1141 - 1152.

Tuazon E.C. and Atkinson R. (1990a) A product study of the gas-phase reaction of methacrolein with the OH radical in the presence of NO_x. *Int. J. Chem. Kinet.* **22**, 591 - 602.

Tuazon E.C. and Atkinson R. (1990b) A product study of the gas-phase reaction of isoprene with the OH radical in the presence of NO_x. *Int. J. Chem. Kinet.* **22**, 1221 - 1236.

Wille U., Becker E., Schindler R.N., Lancar I.T., Poulet G., and Lebras G. (1991) A discharge flow mass-spectrometric study of the reaction between the NO_3 radical and isoprene. *J. Atmos. Chem.* **13**, 183 - 193.

10 Appendix - List of Tables

10.1 Table 1: List of species in RADM-E and RADM-C

1.-63. as in tab. 1 in Stockwell et al. (1990)

additional carbonyls and other stable compounds

64. MAC	methacrolein	$CH_2C(CH_3)CHO$
65. MVK	methyl vinyl ketone	$CH_2CHCOCH_3$
66. MFUR	3-methylfuran	$O(CHCHC(CH3)CH)$
67. HM1	4-hydroxy-2-methyl-2-butenal	$HOCH_2CH(CH_3)CHO$
68. HM2	4-hydroxy-3-methyl-2-butenal	$HOCH_2C(CH_3)CHCHO$
69. DOC		$HOCH_2C(OH)(CH_3)CHO$ + $OHCC(OH)(CH_3)CHO$
70. HALD	glycolaldehyde	$HOCH_2CHO$
71. HKET	hydroxyacetone	$HOCH_2COCH_3$

additional peroxy radicals

72. ISP1	$CH_2C(CH_3)CH(OH)CH_2O_2$
73. ISP2	$CH_2C(CH_3)CH(O_2)CH_2OH$
74. ISP3	$O_2CH_2C(CH_3)CHCH_2OH$
75. ISP4	$HOCH_2C(CH_3)(O_2)CHCH_2$
76. ISP5	$CH_2(O_2)C(CH_3)(OH)CHCH_2$
77. ISP6	$HOCH_2C(CH_3)CHCH_2O_2$
78. ISOP	surrogate for all ISPi in RADM-C
79. MACP	$OHCC(CH_3)(O_2)CH_2OH$ + $OHCC(CH_3)(OH)CH_2O_2$
80. MA2P	$CH_2C(CH_3)C(O)O_2$ (methacrylicperoxy radical)
81. MVKP	$CH_3C(O)CH(O_2)CH_2OH$ + $CH_3C(O)CH(OH)CH_2O_2$
82. MFUP	four peroxyradicals of 3-methylfuran depicted in chapter 2
83. HM1P	$OHCC(CH_3)(O_2)CH(OH)CH_2OH$ + $OHCC(CH_3)(OH)CH(O_2)CH_2OH$
84. HM2P	$OHCCH(O_2)C(CH_3)(OH)CH_2OH$ + $OHCCH(OH)C(CH_3)(O_2)CH_2OH$
85. H1O3	$HOCH_2CHC(CH_3)C(O)O_2$
86. H2O3	$HOCH_2C(CH_3)CHC(O)O_2$
87. DCO3	$HOCH_2C(CH_3)(OH)C(O)O_2$ + $OHCC(CH_3)(OH)C(O)O_2$
88. HALP	$HOCH_2C(O)O_2$
89. HKEP	$HOCH_2C(O)CH_2O_2$ + $HOCH(O_2)C(O)CH_3$

Additional nitrates and PANs

90. ISON	NO_3 - adduct of isoprene
91. MACN	NO_3 - adduct of MAC
92. MVKN	NO_3 - adduct of MVK
93. MFUN	NO_3 - adduct of MFUR
94. MPAN	$CH_2C(CH_3)C(O)O_2NO_2$ (peroxymethacrylic nitric anhydride)
95. IPAN	$HOCH_2C(O)O_2NO_2$ (hydroxy peroxyacetic nitric anhydride)
96. DPAN	$HOCH_2C(CH_3)(OH)C(O)O_2NO_2 + OHCC(CH_3)(OH)C(O)O_2NO_2$
97. HPN1	$HOCH_2CHC(CH_3)C(O)O_2NO_2$
98. HPN2	$HOCH_2C(CH_3)CHC(O)O_2NO_2$

10.2 Table 2: Reactions RADM-E[7]

Photolytic reactions:

```
P1-P22 as in tab. 2a in Stockwell et al. (1990)
P22  HALD -> 2.0 HO2 + HCHO + CO    same photolysis frequency as ALD
```

Thermal reactions:

T1-T124 except T40,T68,T72 as in tab. 2b in Stockwell et al. (1990)

		A	-E/R
T40 ISO + HO	-> 0.12 ISP1 +0.19 ISP2 +0.11 ISP3+	2.55E-11	-409
	-> 0.17 ISP4 + 0.27 ISP5 + 0.14 ISP6		
T68 ISO + NO3	-> ISON	8.00E-13	0
T72 ISO + O3	-> 0.67 MAC + 0.26 MVK + 0.45 O3P+	1.23E-14	-2013
	-> 0.6 HO + 0.8 HCHO + 0.06 HO2 +		
	-> 0.19 CO + 0.06 OLT +		
	-> 0.06 ORA2 + 0.07 ORA1		
T125 MAC + HO	-> 0.5 MACP + 0.5 MA2P	1.86E-11	175
T126 MVK + HO	-> MVKP	4.13E-12	452
T127 HALD + HO	-> 0.8 HALP + 0.2 HO2 + 0.2 GLY	6.87E-12	256
T128 HKET + HO	-> HKEP	3.00E-12	0
T129 MAC + O3	-> 0.91 MGLY + 0.44 O3P + 0.54 HO +	4.40E-15	-2500
	-> 0.8 HCHO + 0.07 ORA1 + 0.09 ORA2		
T130 MVK + O3	-> 0.85 MGLY + 0.44 O3P + 0.42 HO +	4.00E-15	-2000
	-> 0.8 HCHO + 0.07 ORA1 + 0.07 ORA2 +		
	-> 0.08 ALD		
T131 ISP1 + NO	-> 0.17 MFUR + 0.88 NO2 + 0.88 HO2 +	4.20E-12	180
	-> 0.71 HCHO + 0.71 MAC + 0.12 ONIT		
T132 ISP2 + NO	-> 0.88 NO2 + 0.88 HO2 + 0.88 MAC +	4.20E-12	180
	-> 0.12 ONIT + 0.88 HCHO		
T133 ISP3 + NO	-> 0.88 NO2 + 0.88 HO2 + 0.88 HM1	4.20E-12	180
	-> + 0.12 ONIT		
T134 ISP4 + NO	-> 0.18 MFUR + 0.88 NO2 + 0.88 HO2 +	4.20E-12	180
	-> 0.7 HCHO + 0.7 MVK + 0.12 ONIT		
T135 ISP5 + NO	-> 0.88 NO2 + 0.88 HO2 + 0.88 HCHO +	4.20E-12	180
	-> 0.88 MVK + 0.12 ONIT		
T136 ISP6 + NO	-> 0.88 NO2 + 0.88 HO2 + 0.88 HM2	4.20E-12	180
	-> + 0.12 ONIT		
T137 MACP + NO	-> 0.8 HKET + 0.2 HCHO + 0.2 MGLY +	4.20E-12	180
	-> + HO2 + 0.8 CO + NO2		
T138 MA2P + NO	-> NO2 + HCHO + ACO3	4.20E-12	180
T139 MVKP + NO	-> 0.7 ACO3 + 0.7 HALD + 0.3 HCHO	4.20E-12	180
	-> + 0.3 HO2 + 0.3 MGLY + NO2		
T140 HALP + NO	-> NO2 + HO2 + HCHO	4.20E-12	180
T141 HKEP + NO	-> NO2 + 0.5 ORA2 + 0.5 HCHO	4.20E-12	180
	-> + 0.5 HALP + 0.5 HO2		
T142 HM1P + NO	-> NO2 + HO2 + MGLY + HALD	4.20E-12	180
T143 HM2P + NO	-> NO2 + HO2 + GLY + HKET	4.20E-12	180
T144 MFUP + NO	-> NO2 + 0.5 MVK + 0.5 MAC + HO2	4.20E-12	180
T145 DCO3 + NO	-> 0.5 HKET + 0.5 MGLY + HO + NO2	4.20E-12	180

```
T146 ISON + NO     -> 2.0 NO2 + HCHO + 0.5 MVK + 0.5 MAC 4.20E-12  180
T147 MVKN + NO     -> 2.0 NO2 + HCHO + MGLY              4.20E-12  180
T148 MACN + NO     -> 2.0 NO2 + HCHO + MGLY              4.20E-12  180
T149 MFUN + NO     -> 2.0 NO2 + MVK                      4.20E-12  180
T150 HALP + NO2    -> IPAN                               4.7E-12   0
T151 IPAN          -> HALP + NO2                         1.95E+16  -13543
T152 MA2P + NO2    -> MPAN                               4.7E-12   0
T153 MPAN          -> MA2P + NO2                         1.95E+16  -13543
T154 DCO3 + NO2    -> DPAN                               4.7E-12   0
T155 DPAN          -> DCO3 + NO2                         1.95E+16  -13543
T156 DOC + HO      -> DCO3                               1.0E-11   0
T157 ISP1 + HO2    -> OP2                                7.7E-14   1300
T158 ISP2 + HO2    -> OP2                                7.7E-14   1300
T159 ISP3 + HO2    -> OP2                                7.7E-14   1300
T160 ISP4 + HO2    -> OP2                                7.7E-14   1300
T161 ISP5 + HO2    -> OP2                                7.7E-14   1300
T162 ISP6 + HO2    -> OP2                                7.7E-14   1300
T163 HM1P + HO2    -> OP2                                7.7E-14   1300
T164 HM2P + HO2    -> OP2                                7.7E-14   1300
T165 MACP + HO2    -> OP2                                7.7E-14   1300
T166 MA2P + HO2    -> OP2                                7.7E-14   1300
T167 MVKP + HO2    -> OP2                                7.7E-14   1300
T168 HKEP + HO2    -> OP2                                7.7E-14   1300
T169 HALP + HO2    -> OP2                                7.7E-14   1300
T170 MFUP + HO2    -> OP2                                7.7E-14   1300
T171 DCO3 + HO2    -> OP2                                7.7E-14   1300
T172 ISP1 + ISP1   -> 1.2 MAC + 0.6 OLT + 0.2 DCB        2.0E-13   0
                   -> + 1.2 HCHO + 1.2 HO2
T173 ISP1 + ISP2   -> 1.2 MAC + 0.7 OLT + 0.1 DCB +      2.5E-14   0
                   -> 1.2 HCHO + 1.2 HO2
T174 ISP1 + ISP3   -> 0.6 MAC + 0.4 OLT + 0.2 OLI +      2.0E-13   0
                   -> 0.6 HCHO + 1.2 HO2 + 0.8 HM1
T175 ISP2 + ISP3   -> 0.6 MAC + 0.2 OLI + 0.8 HM1 +      2.5E-14   0
                   -> 0.6 HCHO + 1.2 HO2 + 0.3 OLT +
                   -> 0.1 DCB
T176 ISP1 + ISP4   -> 0.6 MAC + 0.6 OLT + 0.2 DCB +      2.0E-13   0
                   -> 1.2 HCHO + 1.2 HO2 + 0.6 MVK
T177 ISP1 + ISP5   -> 0.8 MAC + 0.3 OLT + 0.1 DCB +      4.9E-15   0
                   -> 1.6 HCHO + 1.6 HO2 + 0.8 MVK
T178 ISP1 + ISP6   -> 0.6 MAC + 0.4 OLT + 0.2 OLI +      2.0E-13   0
                   -> 0.6 HCHO + 1.2 HO2 + 0.8 HM2
T179 ISP2 + ISP4   -> 0.6 MAC + 0.6 OLT + 0.2 DCB +      2.5E-14   0
                   -> 1.2 HCHO + 1.2 HO2 + 0.6 MVK
T180 ISP2 + ISP5   -> 0.8 MAC + 0.3 OLT + 0.1 DCB +      1.6E-16   0
                   -> 1.6 HCHO + 1.6 HO2 + 0.8 MVK
T181 ISP2 + ISP6   -> 0.6 MAC + 0.2 OLI + 0.8 HM2 +      2.5E-14   0
                   -> 0.6 HCHO + 1.2 HO2 + 0.3 OLT +
                   -> 0.1 DCB
T182 ISP3 + ISP3   -> 1.6 HM1 + 0.4 OLI + 1.6 HO2        2.0E-13   0
T183 ISP3 + ISP4   -> 0.8 HM1 + 0.6 MVK + 1.2 HO2 +      2.0E-13   0
                   -> 0.6 HCHO + 0.2 OLI + 0.3 OLT +
                   -> 0.1 DCB
T184 ISP3 + ISP5   -> 0.8 MVK + 0.8 HM1 + 1.6 HO2 +      3.1E-16   0
                   -> 0.2 OLI + 0.2 OLT
```

```
T185 ISP3 + ISP6    -> 0.8 HM1 + 0.4 OLI + 0.8 HM2 +      2.0E-13   0
                    -> 1.2 HO2
T186 ISP4 + ISP4    -> 1.2 MVK + 0.6 OLT + 0.2 DCB +      2.0E-13   0
                    -> 1.2 HCHO + 1.2 HO2
T187 ISP4 + ISP5    -> 1.6 MVK + 1.8 HO2 + 1.8 HCHO +     4.9E-15   0
                    -> 0.4 OLT
T188 ISP4 + ISP6    -> 0.6 MVK + 0.8 HM2 + 1.2 HO2 +      2.0E-13   0
                    -> 0.6 HCHO + 0.2 OLI + 0.3 OLT +
                    -> 0.1 DCB
T189 ISP5 + ISP6    -> 0.8 MVK + 0.8 HM2 + 1.6 HO2 +      4.9E-15   0
                    -> 0.2 OLI + 0.2 OLT
T190 ISP6 + ISP6    -> 1.6 HM2 + 0.4 OLI + 1.6 HO2        2.0E-13   0
T191 MACP + ISP1    -> 0.6 MAC + 0.6 MGLY + 1.2 HCHO +    1.0E-13   0
                    -> 1.2 HO2 + 0.4 DOC + 0.1 DCB +
                    -> 0.3 OLT
T192 MACP + ISP3    -> 0.8 HM1 + 0.2 OLI + 0.6 MGLY +     1.0E-13   0
                    -> 0.6 HCHO + 1.2 HO2 + 0.4 DOC
T193 MACP + ISP4    -> 0.6 MVK + 0.6 MGLY + 1.2 HCHO +    1.0E-13   0
                    -> 1.2 HO2 + 0.4 DOC + 0.1 DCB +
                    -> 0.3 OLT
T194 MACP + ISP6    -> 0.8 HM2 + 0.2 OLI + 0.6 MGLY +     1.0E-13   0
                    -> 0.6 HCHO + 1.2 HO2 + 0.4 DOC
T195 MACP + ISP2    -> 0.6 MAC + 0.6 MGLY + 1.2 HCHO +    1.3E-14   0
                    -> 1.2 HO2 + 0.4 DOC + 0.1 DCB +
                    -> 0.3 OLT
T196 MACP + ISP5    -> 0.6 MVK + 0.6 MGLY + 1.2 HCHO +    2.5E-15   0
                    -> 1.2 HO2 + 0.4 DOC + 0.1 DCB +
                    -> 0.3 OLT
T197 MA2P + ISP1    -> 0.8 MAC + 0.2 OLT + 0.2 ORA2 +     8.0E-13   0
                    -> 0.8 ACO3 + 0.8 HO2 + 1.6 HCHO
T198 MA2P + ISP3    -> 0.8 HM1 + 0.2 OLI + 0.2 ORA2 +     8.0E-13   0
                    -> 0.8 ACO3 + 0.8 HO2 + 0.8 HCHO
T199 MA2P + ISP4    -> 0.8 MVK + 0.2 OLT + 0.2 ORA2 +     8.0E-13   0
                    -> 0.8 ACO3 + 0.8 HO2 + 1.6 HCHO
T200 MA2P + ISP6    -> 0.8 HM2 + 0.2 OLI + 0.2 ORA2 +     8.0E-13   0
                    -> 0.8 ACO3 + 0.8 HO2 + 0.8 HCHO
T201 MA2P + ISP5    -> MVK + ACO3 + 2.0 HCHO + HO2        3.0E-15   0
T202 MA2P + ISP2    -> 0.8 MAC + 0.2 OLT + 0.2 ORA2 +     1.6E-14   0
                    -> 0.8 ACO3 + 1.6 HCHO + 0.8 HO2
T203 MVKP + ISP1    -> 0.6 MAC + 0.6 MGLY + 1.2 HCHO +    1.0E-13   0
                    -> 1.2 HO2 + 0.4 DOC + 0.1 DCB +
                    -> 0.3 OLT
T204 MVKP + ISP3    -> 0.8 HM1 + 0.2 OLI + 0.6 MGLY +     1.0E-13   0
                    -> 0.6 HCHO + 1.2 HO2 + 0.4 DOC
T205 MVKP + ISP4    -> 0.6 MVK + 0.6 MGLY + 1.2 HCHO +    1.0E-13   0
                    -> 1.2 HO2 + 0.4 DOC + 0.1 DCB +
                    -> 0.3 OLT
T206 MVKP + ISP6    -> 0.8 HM2 + 0.2 OLI + 0.6 MGLY +     1.0E-13   0
                    -> 0.6 HCHO + 1.2 HO2 + 0.4 DOC
T207 MVKP + ISP2    -> 0.6 MAC + 0.6 MGLY + 1.2 HCHO +    1.3E-14   0
                    -> 1.2 HO2 + 0.4 DOC +0.1 DCB +
                    -> 0.3 OLT
T208 MVKP + ISP5    -> 0.6 MVK + 0.6 MGLY + 1.2 HCHO +    2.5E-15   0
                    -> 1.2 HO2 + 0.4 DOC +0.1 DCB +
                    -> 0.3 OLT
```

T209 MO2 + ISP1	-> 0.5 MAC + 1.25 HCHO + HO2 + -> 0.4 OLT + 0.1 DCB + 0.1 HC3	2.0E-13	0
T210 MO2 + ISP4	-> 0.5 MVK + 1.25 HCHO + HO2 + -> 0.4 OLT + 0.1 DCB + 0.1 HC3	2.0E-13	0
T211 MO2 + ISP3	-> 0.75 HM1 + 0.75 HCHO + HO2 + -> 0.25 OLI + 0.1 HC3	2.0E-13	0
T212 MO2 + ISP6	-> 0.75 HM2 + 0.75 HCHO + HO2 + -> 0.25 OLI + 0.1 HC3	2.0E-13	0
T213 MO2 + ISP2	-> 0.5 MAC + 1.25 HCHO + HO2 + -> 0.4 OLT + 0.1 DCB + 0.1 HC3	2.5E-14	0
T214 MO2 + ISP5	-> 0.7 MVK + 1.7 HCHO + 1.4 HO2 + -> 0.3 OLT	3.1E-16	0
T215 HM1 + HO	-> 0.6 HM1P + 0.4 H1O3	4.0E-11	0
T216 HM2 + HO	-> 0.6 HM2P + 0.4 H2O3	4.0E-11	0
T217 HM1 + O3	-> 0.89 HALD + MGLY + 0.55 O3P + -> 0.68 HO + 0.11 ORA2	1.0E-14	-900
T218 HM2 + O3	-> HKET + 0.89 GLY + 0.55 O3P + -> 0.68 HO + 0.11 ORA2	1.0E-14	-900
T219 HM1 + NO3	-> OLN	5.0E-13	0
T220 HM2 + NO3	-> OLN	5.0E-13	0
T221 MAC + NO3	-> 0.3 HNO3 + 0.3 MA2P + 0.7 MACN	1.0E-14	0
T222 MVK + NO3	-> MVKN	6.0E-14	0
T223 HALD + NO3	-> HNO3 + HALP	5.2E-16	0
T224 HKET + NO3	-> HNO3 + HKEP	1.0E-16	0
T225 MFUR + HO	-> MFUP	9.4E-11	0
T226 MFUR + NO3	-> MFUN	1.0E-13	0
T227 DOC + NO3	-> DCO3 + HNO3	5.0E-15	0
T228 H1O3 + NO2	-> HPN1	4.7E-12	0
T229 H2O3 + NO2	-> HPN2	4.7E-12	0
T230 HPN1	-> H1O3 + NO2	1.95E+16	-13543
T231 HPN2	-> H2O3 + NO2	1.95E+16	-13543
T232 H1O3+ NO	-> HALD + ACO3 + NO2	4.2E-12	180
T233 H2O3+ NO	-> HKET + CO + HO2 + NO2	4.2E-12	180
T234 H1O3+ HO2	-> OP2	7.7E-14	1300
T235 H2O3+ HO2	-> OP2	7.7E-14	1300

[1] The trace gases H_2O, CO_2, H_2, O_2, and N_2 are only treated as products.

10.3 Table 3: Reactions of RADM-C*

Photolytic reactions:
see table 2.

Thermal reactions:
T1-T124 except T40,T68,T72 as in tab. 2b in Stockwell et al. (1990)

T40 ISO + HO	-> ISOP	2.55E-11	409
T68 ISO + NO3	-> ISON	8.00E-13	0
T72 ISO + O3	-> 0.67 MAC + 0.26 MVK + 0.45 O3P +	1.23E-14	-2013
	-> 0.60 HO + 0.8 HCHO + 0.06 HO2 +		
	-> 0.19 CO + 0.06 OLT + 0.06 ORA2 +		
	-> 0.07 ORA1		
T125 MAC + HO	-> 0.6 MACP + 0.4 ACO3 + 0.4 HCHO	1.86E-11	175
T126 MVK + HO	-> MVKP	4.13E-12	452
T127 HALD + HO	-> 0.4 MO2 + 0.6 HO2 + 0.2 GLY	6.87E-12	256
T128 HKET + HO	-> 0.9 MO2 + 0.1 HO2 + 0.5 HCHO +	3.00E-12	0
	-> 0.5 ORA2		
T129 MAC + O3	-> 0.91 MGLY + 0.44 O3P + 0.54 HO +	4.40E-15	-2500
	-> 0.8 HCHO + 0.07 ORA1 + 0.09 ORA2		
T130 MVK + O3	-> 0.85 MGLY + 0.44 O3P + 0.42 HO +	4.00E-15	-2000
	-> 0.8 HCHO + 0.07 ORA1 + 0.07 ORA2 +		
	-> 0.08 ALD		
T131 ISOP + NO	-> 0.88 NO2 + 0.88 HO2 + 0.38 MVK +	4.20E-12	180
	-> 0.28 MAC + 0.62 HCHO + 0.1 GLY +		
	-> 0.09 MGLY + 0.02 ORA2 + 0.12 ONIT +		
	-> 0.09 HALD + 0.12 HKET + 0.11 HO		
T132 MACP + NO	-> 0.8 HKET + 0.2 HCHO + 0.2 MGLY +	4.20E-12	180
	-> HO2 + NO2		
T133 MVKP + NO	-> 0.7 ACO3 + 0.7 HALD + 0.3 HCHO +	4.20E-12	180
	-> 0.3 HO2 + 0.3 MGLY + NO2		
T134 ISON + NO	-> 2.0 NO2 + HCHO + 0.5 MVK +	4.20E-12	180
	-> 0.5 MAC		
T135 ISOP + HO2	-> OP2	7.7E-14	1300
T136 MACP + HO2	-> OP2	7.7E-14	1300
T137 MVKP + HO2	-> OP2	7.7E-14	1300
T138 ISOP + ISOP	-> 0.37 MAC + 0.5 MVK + 0.3 OLT +	1.0E-13	0
	-> 0.06 DCB + 0.1 OLI + 1.6 HO2 +		
	-> 0.5 HCHO + 0.18 GLY + 0.16 MGLY +		
	-> 0.16 HALD + 0.22 HKET + 0.2 HO +		
	-> 0.04 ORA2		
T139 MVK+NO3	-> NO2 + MVKP	6.0E-14	0
T140 MAC+NO3	-> 0.3 HNO3 + 0.7 NO2 + 0.7 MACP +	1.0E-14	0
	-> 0.3 TCO3		
T141 MVKP+ISOP	-> 0.3 MAC + 0.3 MVK + 0.6 MGLY +	5.0E-14	0
	-> HCHO + 1.2 HO2 + 0.1 DCB +		
	-> 0.4 OLT + 0.3 OLI		
T142 MACP + ISOP	-> 0.3 MAC + 0.3 MVK + 0.6 MGLY +	5.0E-14	0
	-> HCHO + 1.2 HO2 + 0.1 DCB +		
	-> 0.4 OLT + 0.3 OLI		

*) The trace gases H_2O, CO_2, H_2, O_2, and N_2 are only treated as products.

10.4 Table 4: Initial conditions for the model runs

10.4.1 Table 4a: Initial mixing ratios

Initial mixing ratios of the lower box in ppb, upper box in brackets. Fixed mixing ratios are denoted by *. Scenarios (see sec 4) : 1 (remote case), 2 (rural case), 3 (suburban case), 4 (urban case). Arbitrary low initial values are assigned to the steady state substances (NO3, N2O5, HONO, HNO4, OH, HO2, all RO2) and biogenic substances (MAC, MVK, HALD, HKET, HM1, HM2, MFUR, MPAN, IPAN, DPAN, DOC). HNO3, ORA1, ORA2, ONIT = 0.

Pressure = 1 atm, H2O mixing ratio is 0.03 in scenario 1

and 0.01 in scenarios 2 - 4.

scenario:	1	2	3	4
NO2	2.0E-4(1.0E-3)	1 (0.5)	3 (1)	50 (10)
NO	1.0E-4(5.0E-4)	0.5 (0.2)	1.5 (0.5)	20 (4)
O3	40 (60)	60 (60)	90 (80)	100 (80)
SO2	0.01 (0)*	0.01 (0)*	0.01 (0)*	0.01 (0)*
CO	100 (100)*	150 (150)*	200 (200)*	400 (200)
CH4	1.7E+3(1.7E+3)*	1.7E+3(1.7E+3)*	1.7E+3(1.7E+3)*	2.0E+3(2.0E+3)*
ETH	1 (1)*	1.5 (1.5)*	2 (2)*	5 (2)
HC3	1 (1)*	1 (1)*	2 (1)*	0.1 (1)
HC5	0 (0)*	0.5 (0.5)*	1 (0.5)*	5 (0.5)
HC8	0 (0)*	0 (0)*	0.1 (0.01)*	1 (0.01)
OL2	0.1 (0.1)*	0.5 (0.5)*	1 (0.5)*	2 (0.5)
OLT	0.1 (0.1)	0.1 (0.1)	0.1 (0.1)	0.1 (0.1)
OLI	0 (0)	0 (0)	0 (0)	0 (0)
ISO	0.1 (0)	0.1 (0)	0.1 (0)	0.1 (0)
TOL	0 (0)*	0.01 (0.01)*	0.1 (0.01)*	0.1 (0.01)
CSL	0 (0)*	1.0E-3 (1.0E-3)*	1.0E-3 (1.0E-3)*	1.0E-3 (1.0E-3)
XYL	0 (0)*	0.01 (0.01)*	0.1 (0.01)*	0.1 (0.01)
HCHO	0.01 (0.01)	0.1 (0.1)	0.1 (0.1)	0.1 (0.1)
ALD	0.01 (0.01)	0.1 (0.1)	0.1 (0.1)	0.1 (0.1)
KET	0.01 (0.01)	0.1 (0.1)	0.1 (0.1)	0.1 (0.1)
GLY	0.01 (0.01)	0.01 (0.01)	0.01 (0.01)	0.01 (0.01)
MGLY	0.01 (0.01)	0.01 (0.01)	0.01 (0.01)	0.01 (0.01)
PAN	0.01 (0.01)	0.01 (0.01)	0.01 (0.01)	0.01 (0.01)
TPAN	0 (0)	0 (0)	0 (0)	0 (0)
PAA	1.0E-3 (0)	1.0E-3 (0)	1.0E-3 (0)	1.0E-3 (0)
DCB	0.01 (0.01)	0.01 (0.01)	0.01 (0.01)	0.01 (0.01)
H2O2	1.0E-3 (1.0E-3)	1.0E-3 (1.0E-3)	1.0E-3 (1.0E-3)	1.0E-3 (1.0E-3)
OP1	0.01 (0)	0.01 (0)	0.01 (0)	0.01 (0)
OP2	0.01 (0)	0.01 (0)	0.01 (0)	0.01 (0)

10.4.2 Table 4b: Source strengths of various trace gases

Source strengths of various trace gases in $cm^{-2}s^{-1}$. Fixed mixing ratios are denoted by *. Scenarios: 1 (remote case), 2 (rural case), 3 (suburban case), 4 (urban case)

scenario:	1	2	3	4
NO	2.0E+09	2.0E+10	see text	1.0E+12
CO	*	*	*	8.0E+12
ETH	*	*	*	2.0E+10
HC3	*	*	*	2.0E+11
HC5	*	*	*	2.0E+11
HC8	*	*	*	1.0E+11
OL2	*	*	*	3.0E+11
OLT	2.0E+04	2.0E+06	2.0E+06	1.0E+12
OLI	0	0	0	1.0E+12
ISO	see text			
TOL	*	*	*	4.0E+10
CSL	*	*	*	2.0E+10
XYL	*	*	*	4.0E+10

10.4.3 Table 4c: Deposition velocities in cm/s.

NO_2	0
N_2O_5	1
HNO_3	1
O_3	0.5
H_2O_2	0.1
HCHO	0.5
ALD	0.5
KET	0.5
GLY	0.5
MGLY	0.5
DCB	0.5
PAN	0.2
TPAN	0.2
OP1	0.1
OP2	0.1
PAA	0.5
ORA1	1
ORA2	1

10.5 Table 5: Results of the model runs for the last day of simulation

15.00 LT (75 hours after model start) (mixing ratios in ppb, OH and HO_2: concentrations in 10^6 cm^{-3} and 10^8 cm^{-3}). The scenarios are denoted by numbers 1 (remote), 2 (rural), 3 (suburban), 4 (urban). The mechanisms are denoted by letters A (RADM2), B (RADM-E), C (RADM-C), L (LLA).

	remote			remote				suburban				urban		
	A	E	C	A	E	C	L	A	E	C	L	A	E	C
NO_2	0.09	3E-3	3E-3	0.65	0.12	0.12	0.11	5.08	3.43	3.64	2.68	8.40	7.43	7.70
ONIT	0.01	0.13	0.13	0.05	0.93	0.95	-	0.42	2.36	2.35	-	3.56	5.08	5.09
PAN	4E-3	5E-4	5E-4	0.12	0.05	0.05	0.13	2.08	1.80	1.92	2.00	14.9	14.2	14.8
HNO_3	0.02	8E-3	9E-3	0.25	0.10	0.11	0.07	15.4	14.9	15.2	14.5	10.2	9.53	9.77
O_3	37	35	36	65	60	61	58	100	109	111	113	210	211	213
HO	0.25	0.29	0.28	0.73	0.45	0.46	0.26	5.25	4.95	5.39	4.03	5.05	4.82	5.02
HO_2	1.87	.82	1.55	3.44	3.63	3.71	3.71	4.35	6.99	7.00	8.82	11.5	13.0	13.1
H_2O_2	0.31	0.18	0.26	0.50	0.68	0.74	0.78	0.28	0.84	0.91	1.40	5.45	6.35	6.44
OP1	0.07	0.05	0.05	0.09	0.08	0.09	0.43	0.05	0.10	0.13	0.12	1.18	1.33	1.38
OP2	0.35	2.81	2.52	0.49	2.10	1.92	0.48	0.11	0.55	0.48	0.03	1.75	2.62	2.49
HCHO	1.56	1.64	1.59	4.52	3.66	3.72	3.79	10.7	9.71	9.99	11.7	25.8	25.7	26.3
ALD	2.39	0.39	0.35	6.02	0.42	0.39	0.24	8.26	0.66	0.66	0.51	21.9	14.9	14.7
GLY	4E-7	0.15	0.13	1E-3	0.31	0.30	0.01	0.03	1.31	1.36	0.04	0.24	1.24	1.27
MGLY	2E-5	0.12	0.10	7E-4	0.25	0.25	4E-4	0.03	0.77	0.78	0.04	0.15	1.00	1.01
ISO	13.6	13.7	13.7	8.55	10.8	10.6	12.4	2.29	2.38	2.19	2.79	2.15	2.24	2.17
MAC	-	1.91	2.06	-	2.77	2.79	2.78	-	1.71	1.62	2.88	-	2.24	2.23
MVK	-	1.25	1.47	-	2.64	2.69	2.61	-	2.92	2.78	3.55	-	2.91	2.90
HALD	-	0.28	0.29	-	0.82	0.91	0.28	-	1.96	1.98	1.20	-	1.66	1.77
HKET	-	0.48	0.46	-	1.39	1.30	-	-	3.31	3.07	-	-	3.01	2.88

10.6 Table 6: Performance of RADM-C

Mean normalized bias b and standard deviations σ and extrema of the deviations (minimum of c_c/c_e = min, maximum = max). The scenarios are denoted by numbers 1 (remote), 2 (rural), 3 (suburban), 4 (urban).

	Scenario 1:				Scenario 2:			
	min	max	σ	b	min	max	σ	b
NO_2	0.96	1.37	0.29	-0.23	0.93	1.09	0.04	-0.03
O_3	1.00	1.01	0.09	-0.007	1.01	1.10	0.03	-0.02
H_2O_2	1.21	1.41	0.34	-0.35	1.06	1.15	0.10	-0.08
HO	0.96	1.21	0.10	-0.03	0.99	1.53	0.44	-0.21
HO_2	0.91	1.96	0.78	-0.47	1.00	1.48	0.10	-0.06
HCHO	0.94	1.09	0.03	0.01	1.00	1.24	0.10	-0.04
PAN	0.97	3.35	0.83	-0.61	0.94	2.15	0.54	-0.35

	Scenario 3:				Scenario 4:			
	min	max	σ	b	min	max	σ	b
NO_2	0.95	1.06	0.034	0.009	0.99	1.04	0.005	-0.002
O_3	0.95	1.03	0.020	-0.009	0.96	1.07	0.010	-0.007
H_2O_2	1.02	1.17	0.044	-0.04	1.00	1.01	0.010	-0.01
HO	0.90	1.18	0.20	-0.09	1.00	1.04	0.034	0.02
HO_2	0.88	1.17	0.10	-0.03	1.00	1.01	0.015	-0.007
HCHO	0.82	1.10	0.05	0.02	0.98	1.02	0.010	-0.005
PAN	0.92	1.59	0.20	-0.15	0.97	1.04	0.020	-0.01

10.7 Table 7: Yields for several products in RADM-E

Yields for several products in RADM-E from the isoprene degradation on a molecule-by-molecule basis [1] :

HCHO	2.07
CO	2.89 [2]
ONIT	0.12
ORA2	0.116
CO2	1.31
PAN	0.65
MPAN	0.14
PAN analogues	0.09

[1] Only the reactions with HO and NO are taken into account. Degradation by ozone and permutation reactions of the peroxy radicals are not considered.

[2] Subsequent contributions from HCHO are included.

11 Figure captions

Fig. 1: Diurnal cycle of the isoprene-flux. Time is local time.

Fig. 2: Diurnal cycles of mixing ratios of some species in the scenario 2 (rural case). Full line is RADM2, broken line is RADM-E, and dotted line is RADM-C.

Fig. 3: Diurnal cycles of mixing ratios of some species in the scenario 3 (suburban case). Full line is RADM2, broken line is RADM-E, and dotted line is RADM-C.

Fig. 4: Diurnal cycles of mixing ratios of some species in scenario 2 (rural case). Full line is RADM-E, dotted line is LLA.

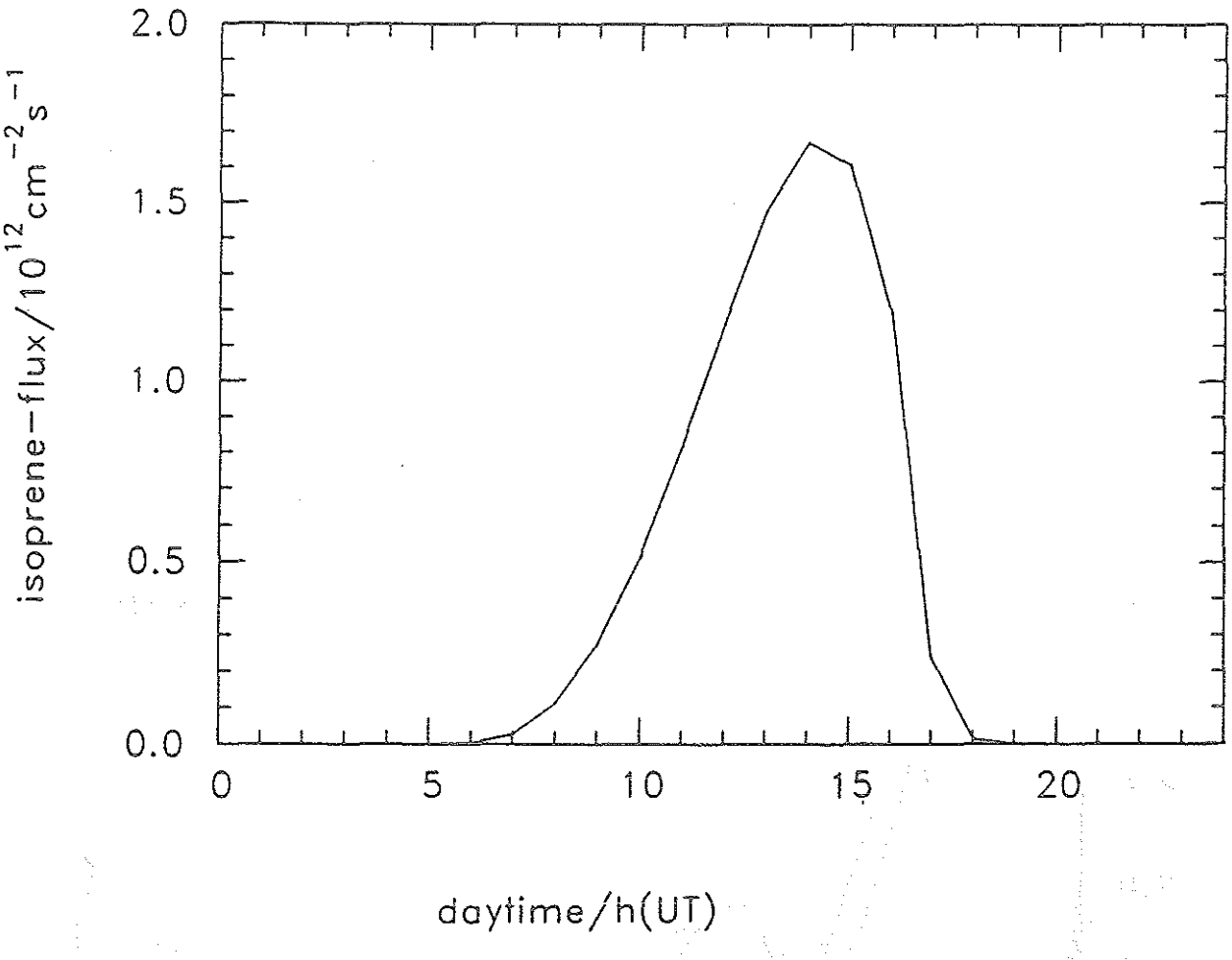

Fig. 1

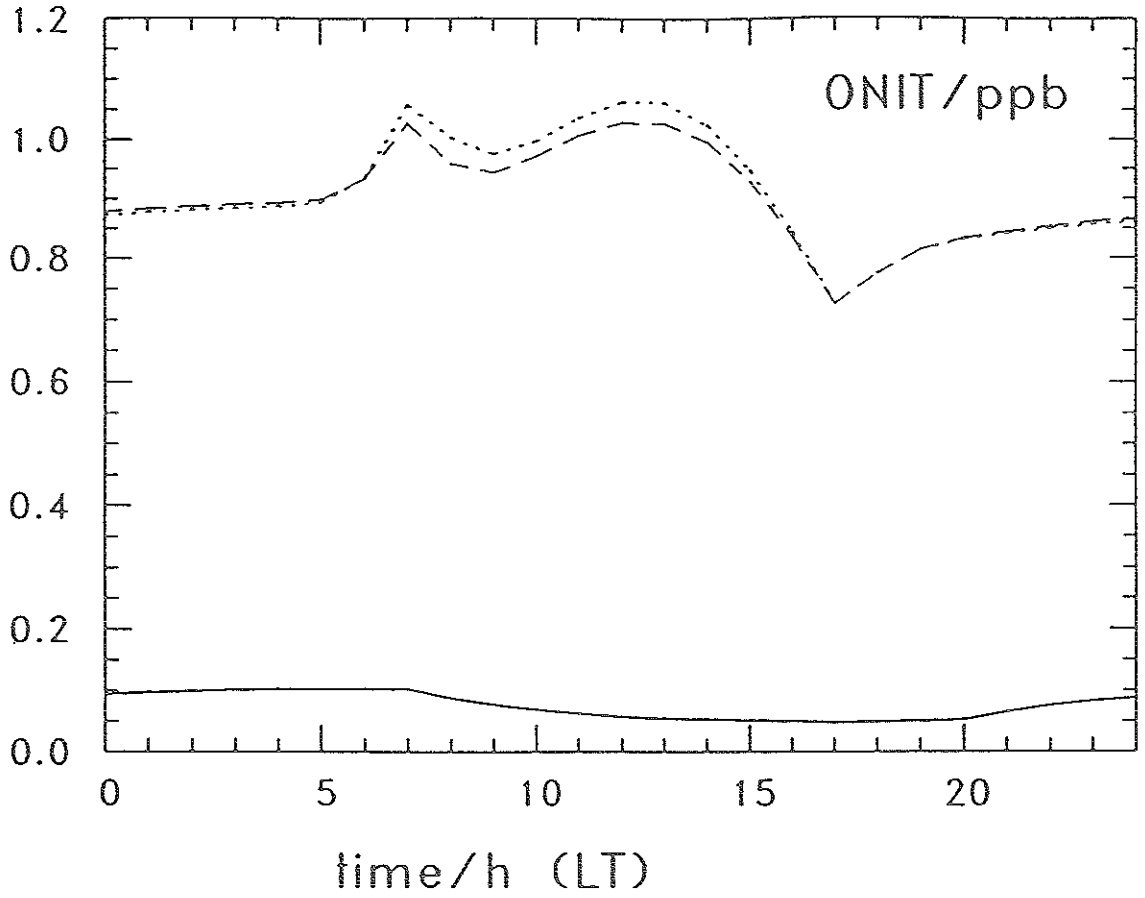
1.2
1.0
0.8
0.6
0.4
0.2
0.0
ONIT/ppb
0
5
10
15
20
time/h (LT)

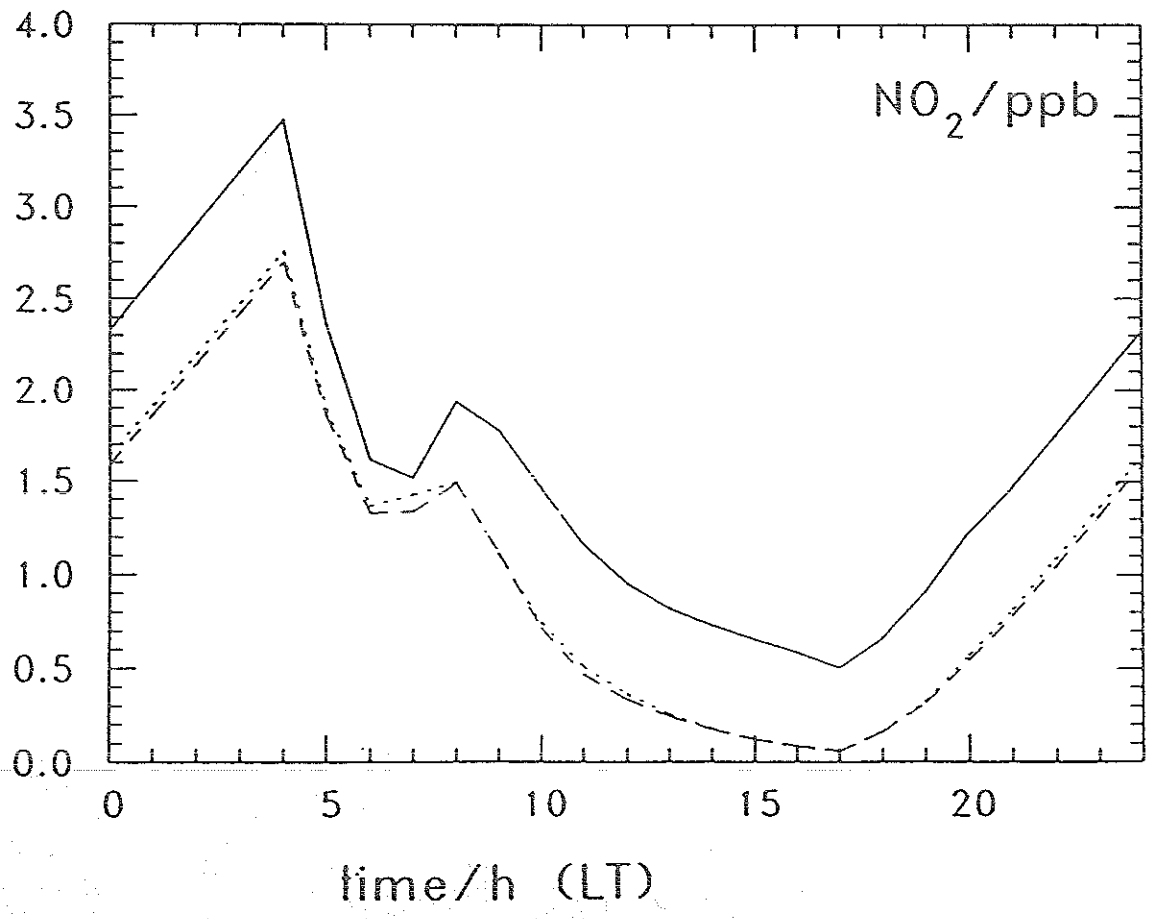
4.0
3.5
3.0
2.5
2.0
1.5
1.0
0.5
0.0
NO2/ppb
0
5
10
15
20
time/h (LT)

Fig. 2a, 2b

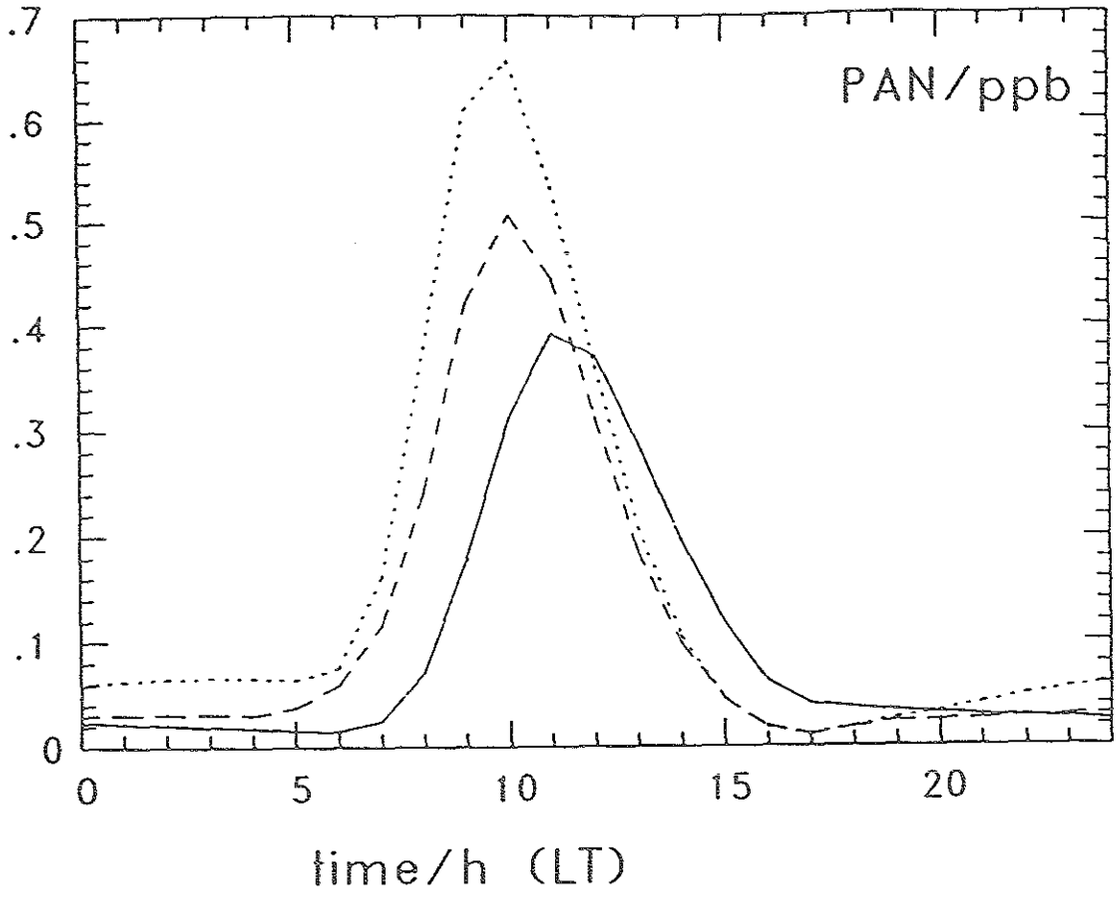
.7
.6
.5
.4
.3
.2
.1
0
PAN/ppb
0
5
10
15
20
time/h (LT)

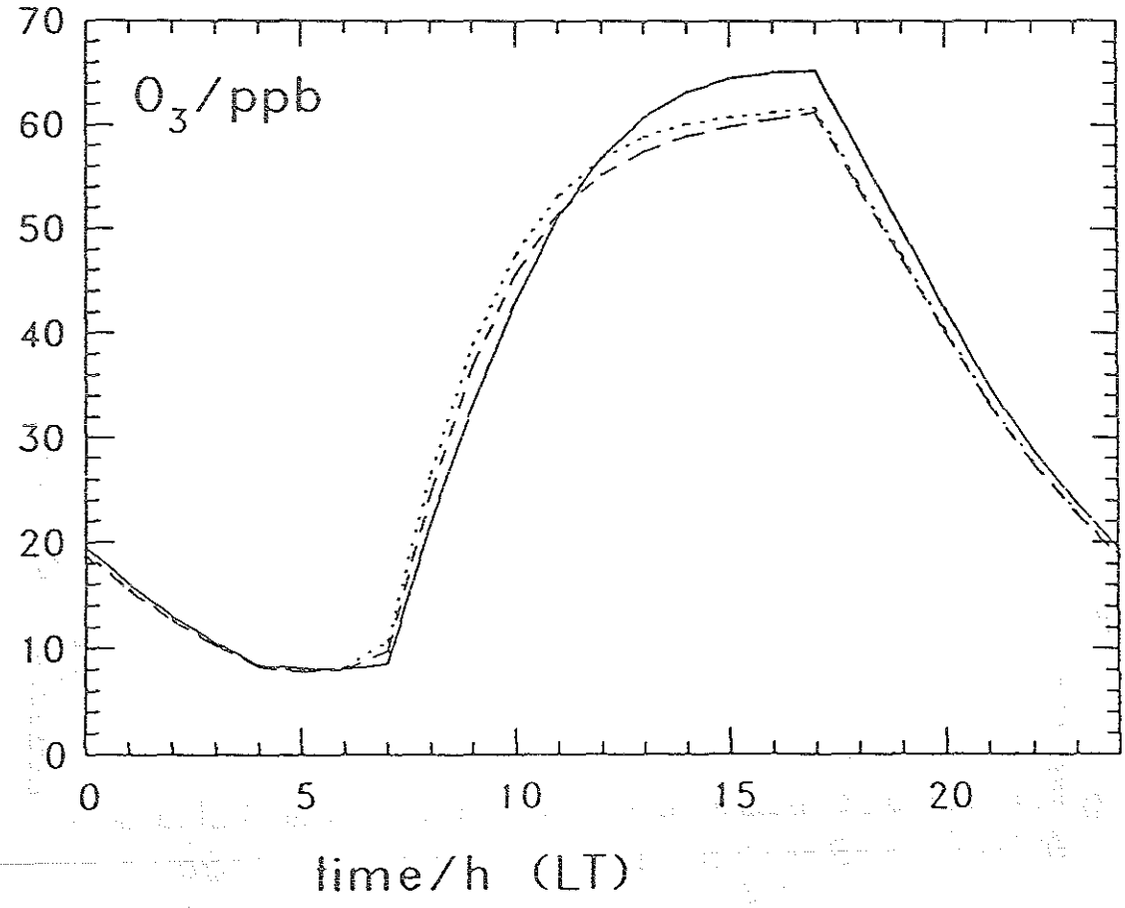
70
60
50
40
30
20
10
0
O_3/ppb
0
5
10
15
20
time/h (LT)

Fig. 2c, 2d

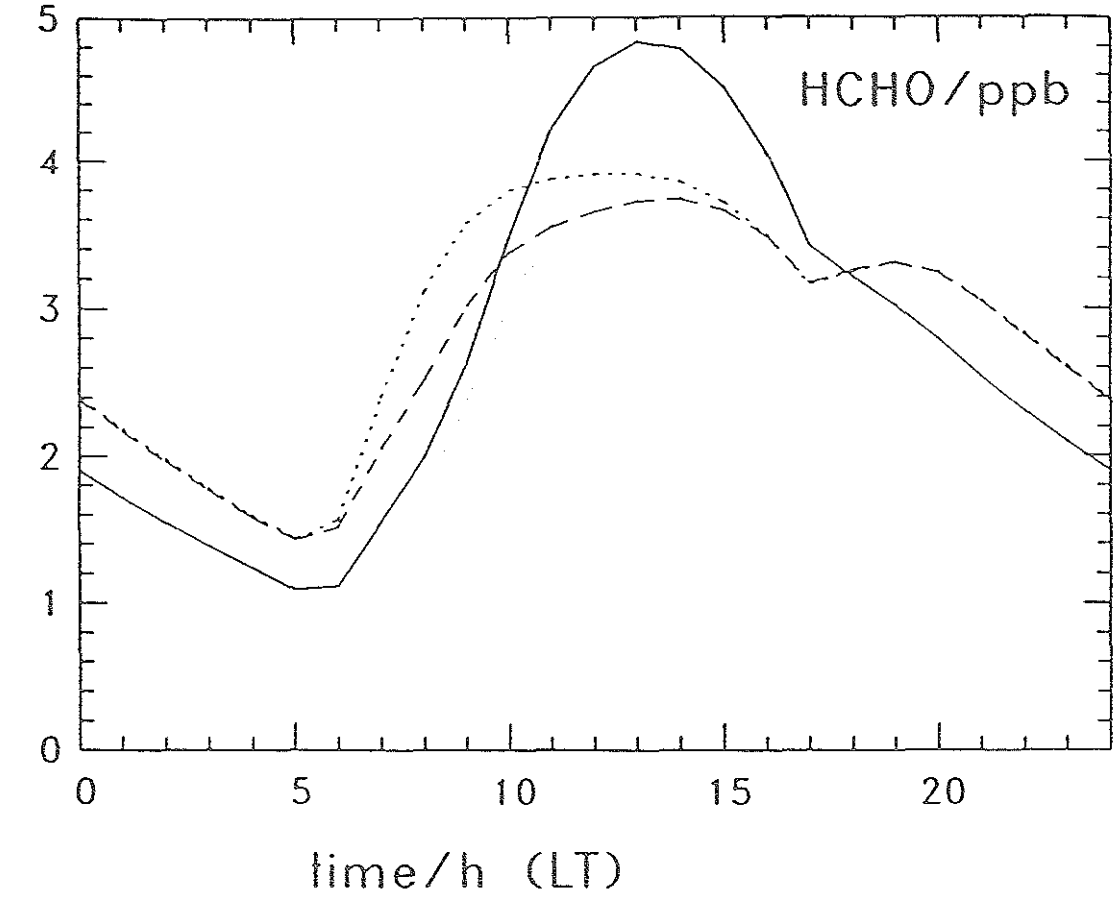
HCHO/ppb
5
4
3
2
1
0
0
5
10
15
20
time/h (LT)

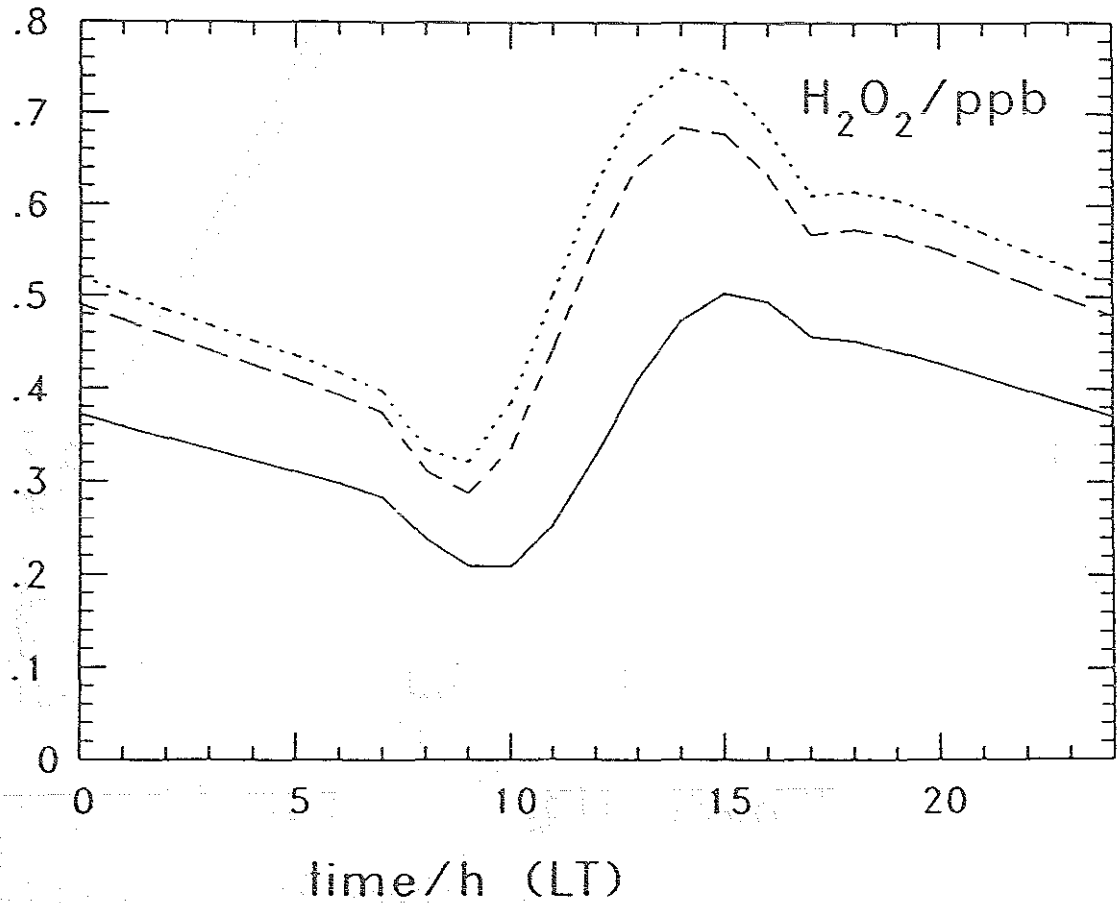
H_2O_2/ppb
.8
.7
.6
.5
.4
.3
.2
.1
0
0
5
10
15
20
time/h (LT)

Fig. 2e, 2f

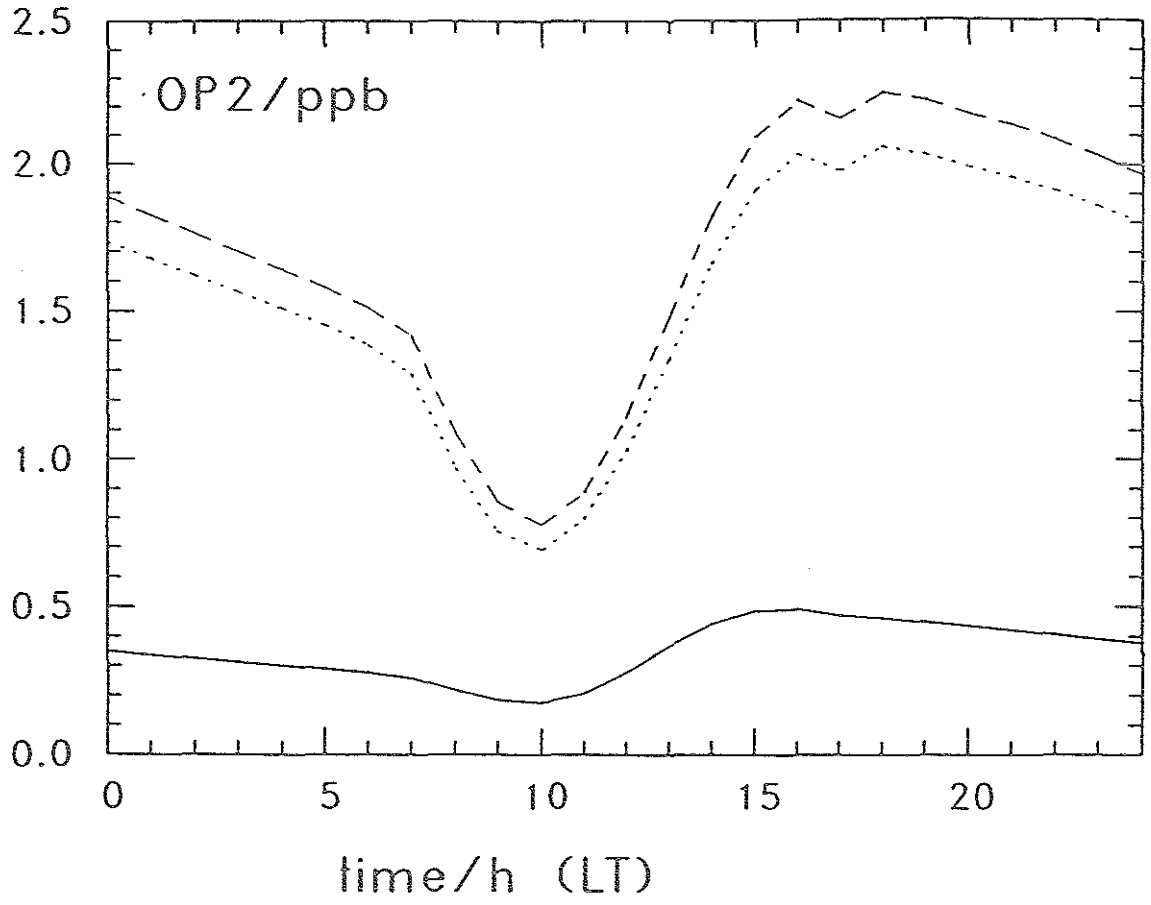
OP2/ppb
2.5
2.0
1.5
1.0
0.5
0.0
0
5
10
15
20
time/h (LT)

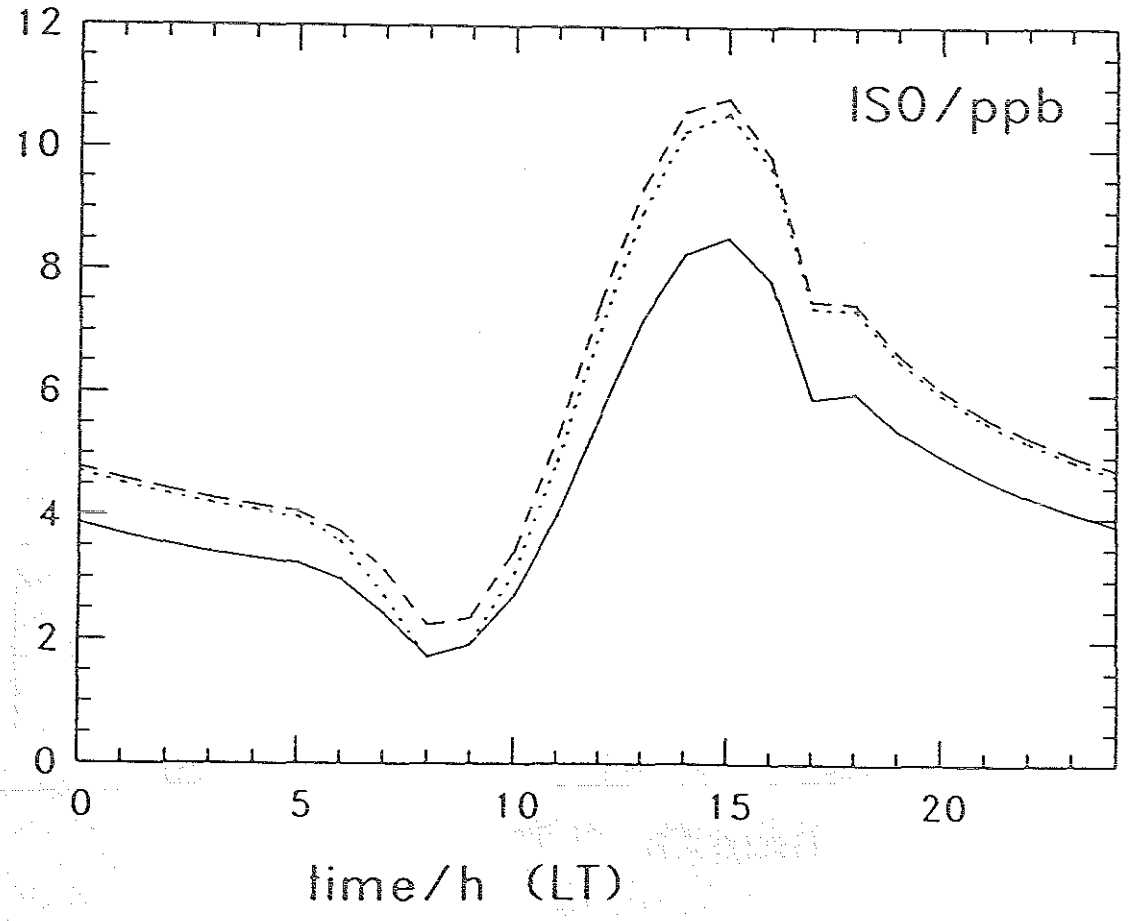
ISO/ppb
12
10
8
6
4
2
0
0
5
10
15
20
time/h (LT)

Fig. 2g, 2h

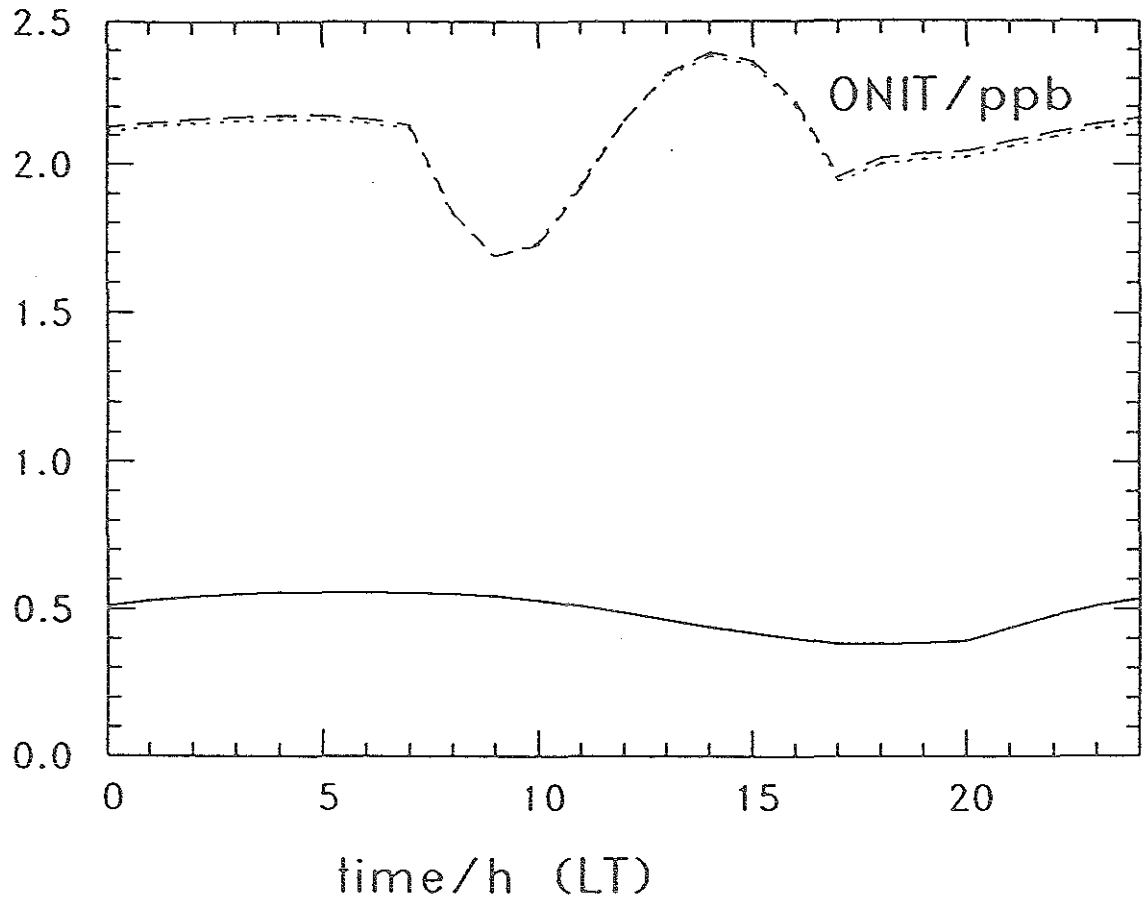
2.5
2.0
1.5
1.0
0.5
0.0
ONIT/ppb
0
5
10
15
20
time/h (LT)

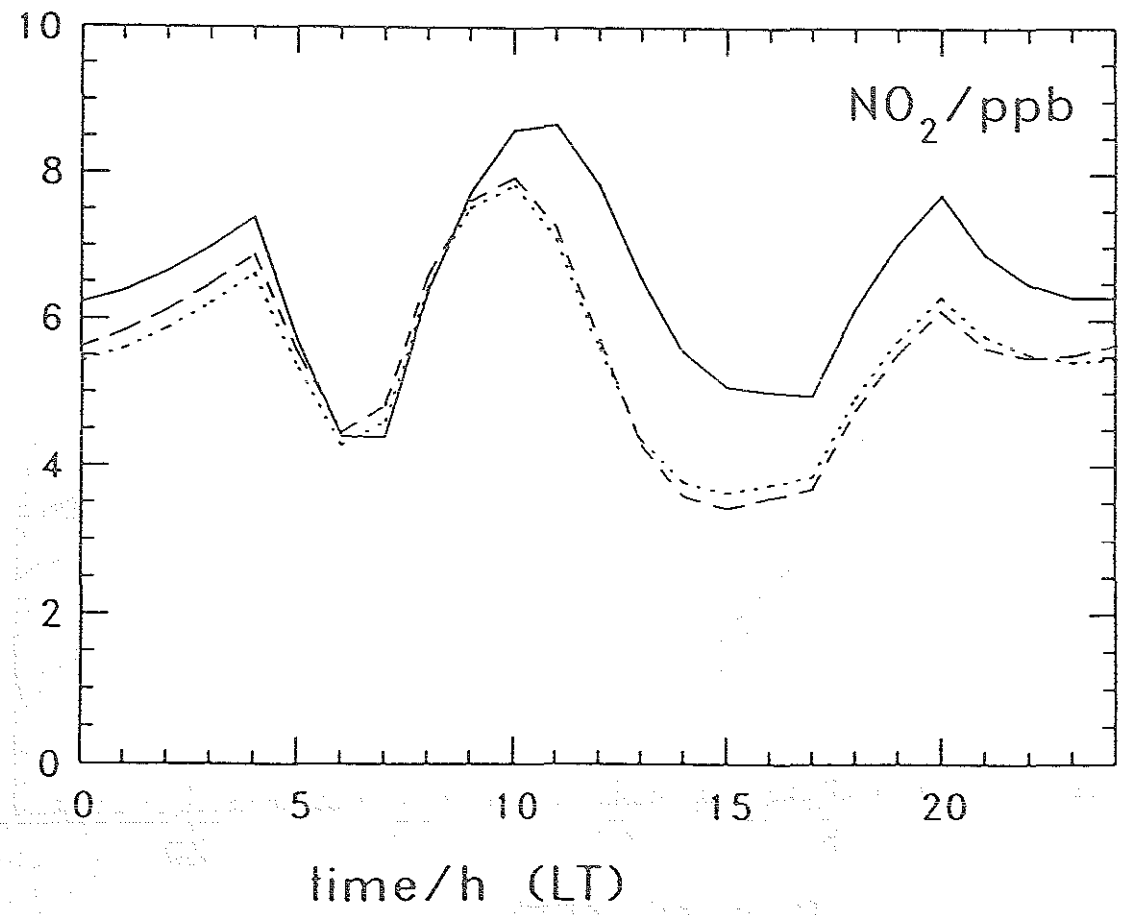
10
8
6
4
2
0
NO2/ppb
0
5
10
15
20
time/h (LT)

Fig. 3a, 3b

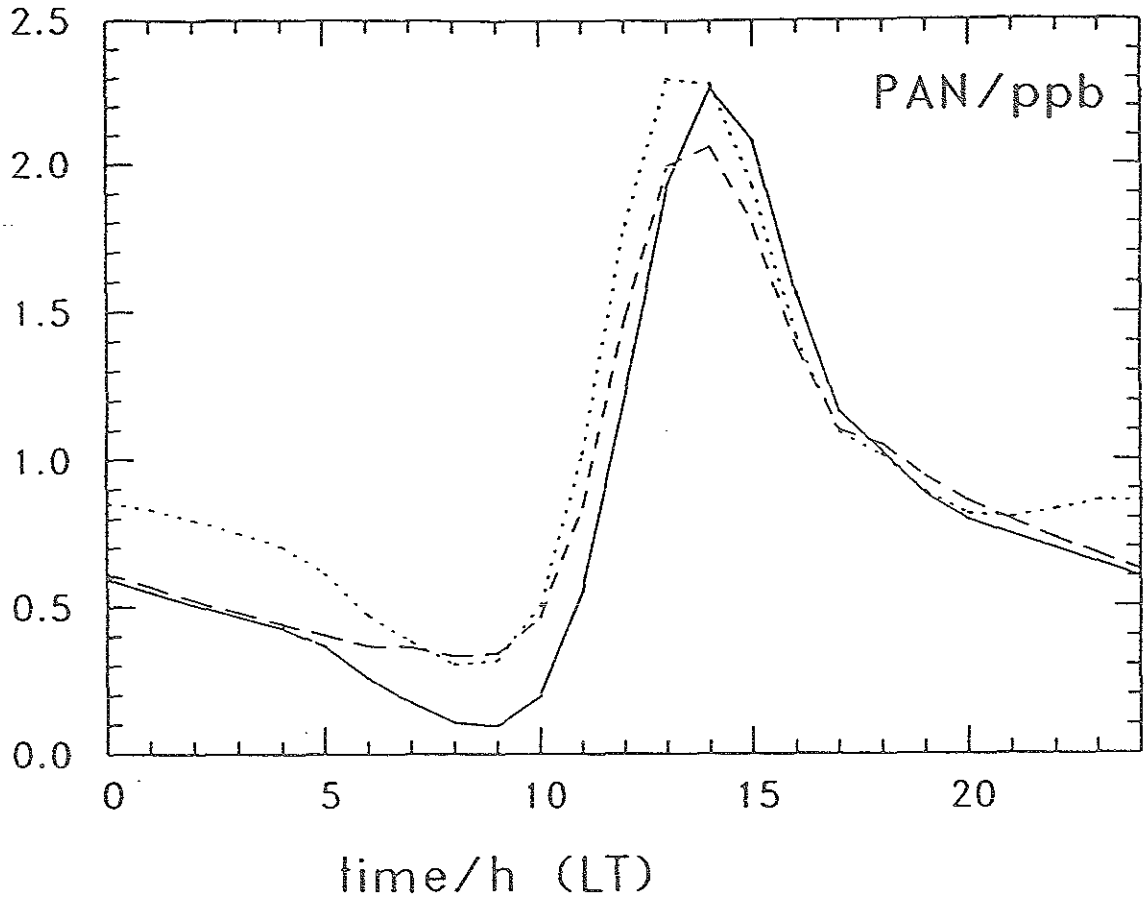
PAN/ppb
2.5
2.0
1.5
1.0
0.5
0.0
0
5
10
15
20
time/h (LT)

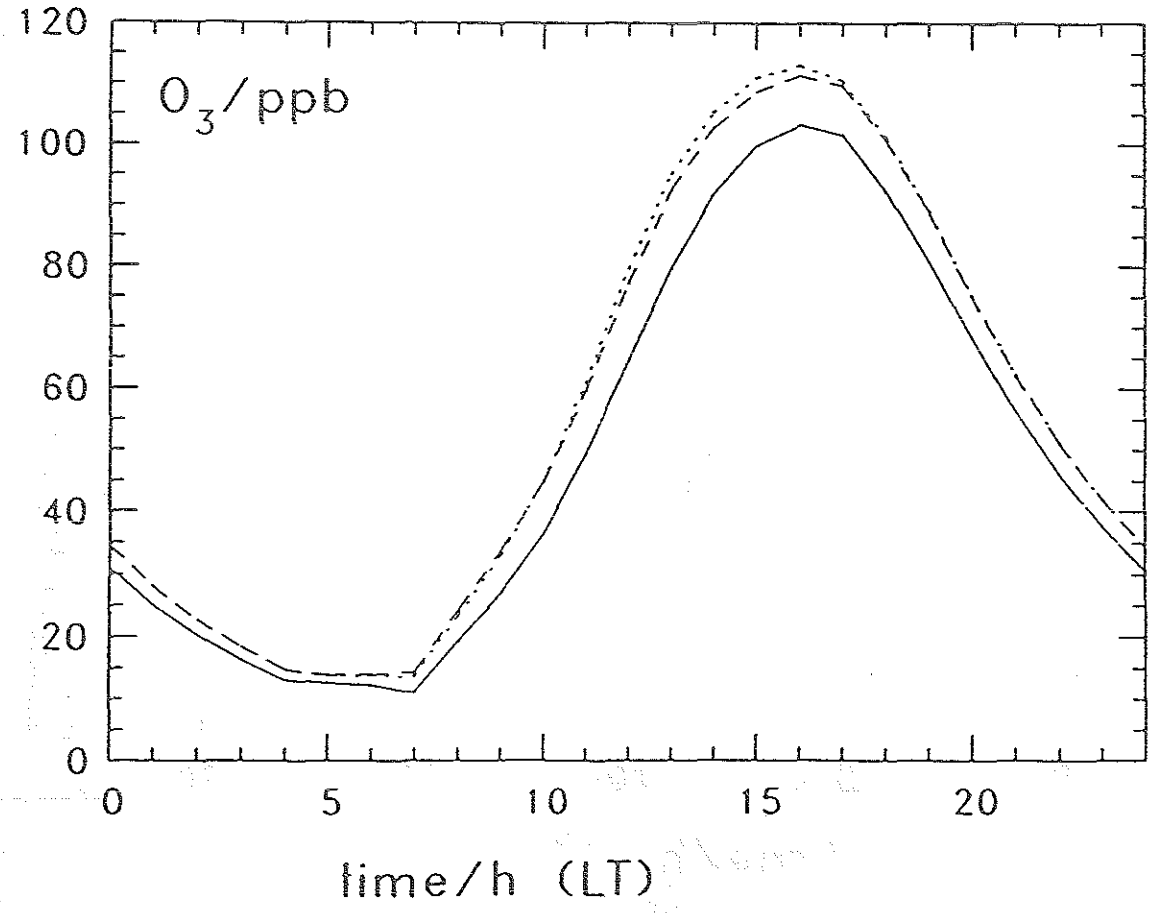
O3/ppb
120
100
80
60
40
20
0
0
5
10
15
20
time/h (LT)

Fig. 3c, 3d

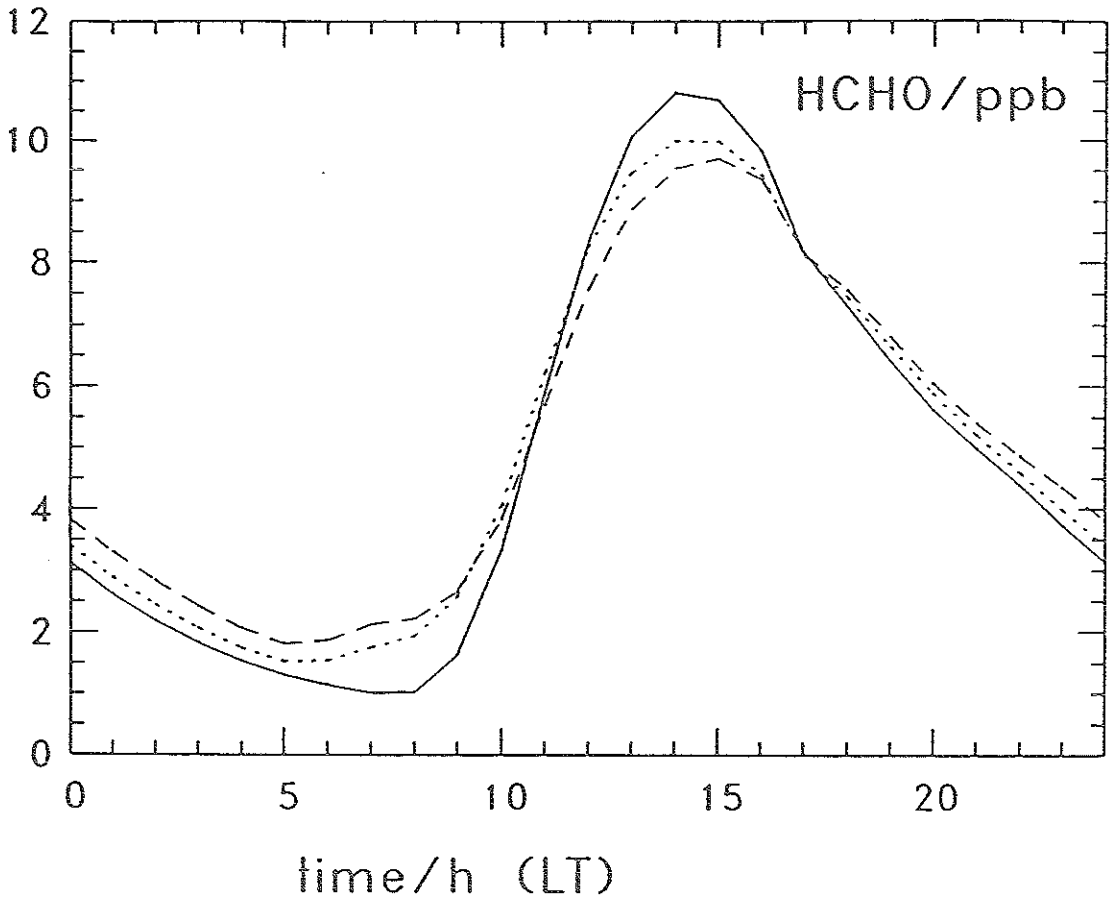
HCHO/ppb
12
10
8
6
4
2
0
0
5
10
15
20
time/h (LT)

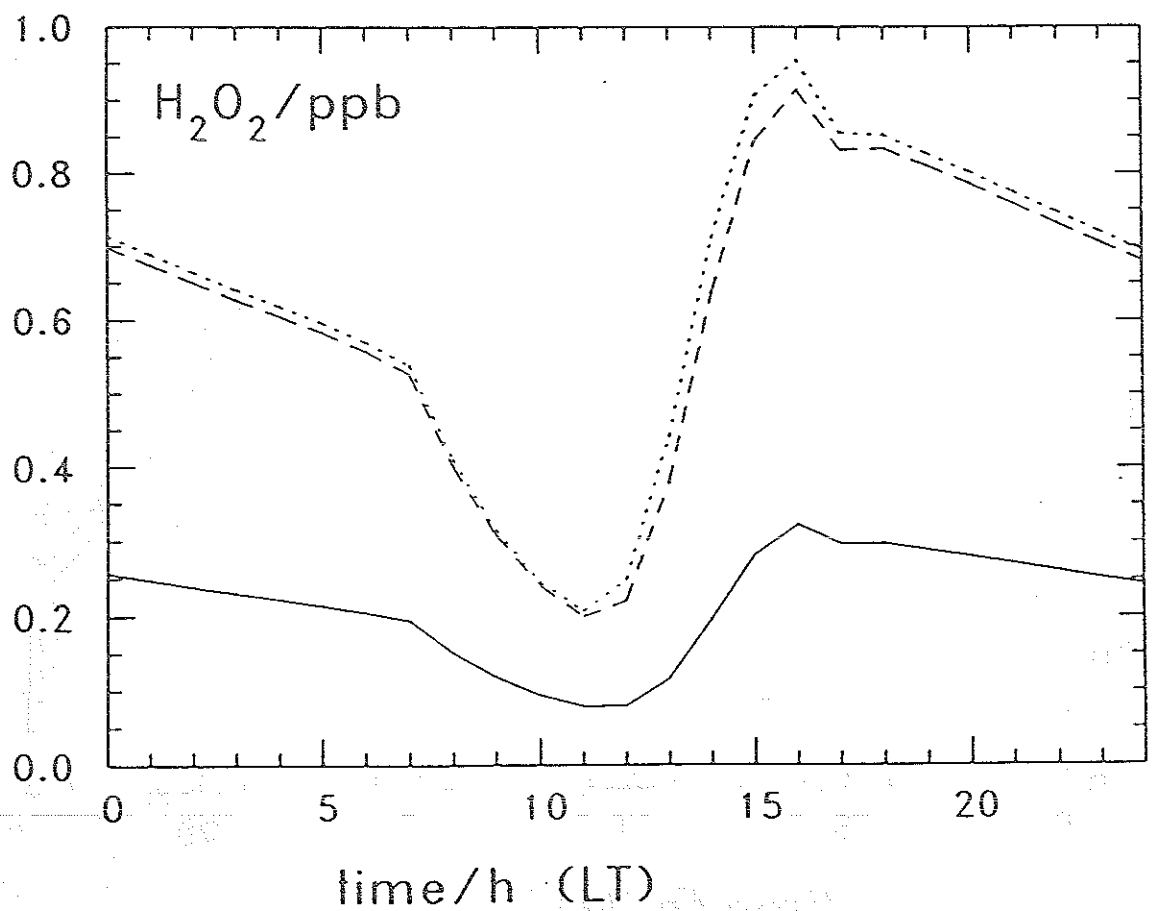
H_2O_2/ppb
1.0
0.8
0.6
0.4
0.2
0.0
0
5
10
15
20
time/h (LT)

Fig. 3e, 3f

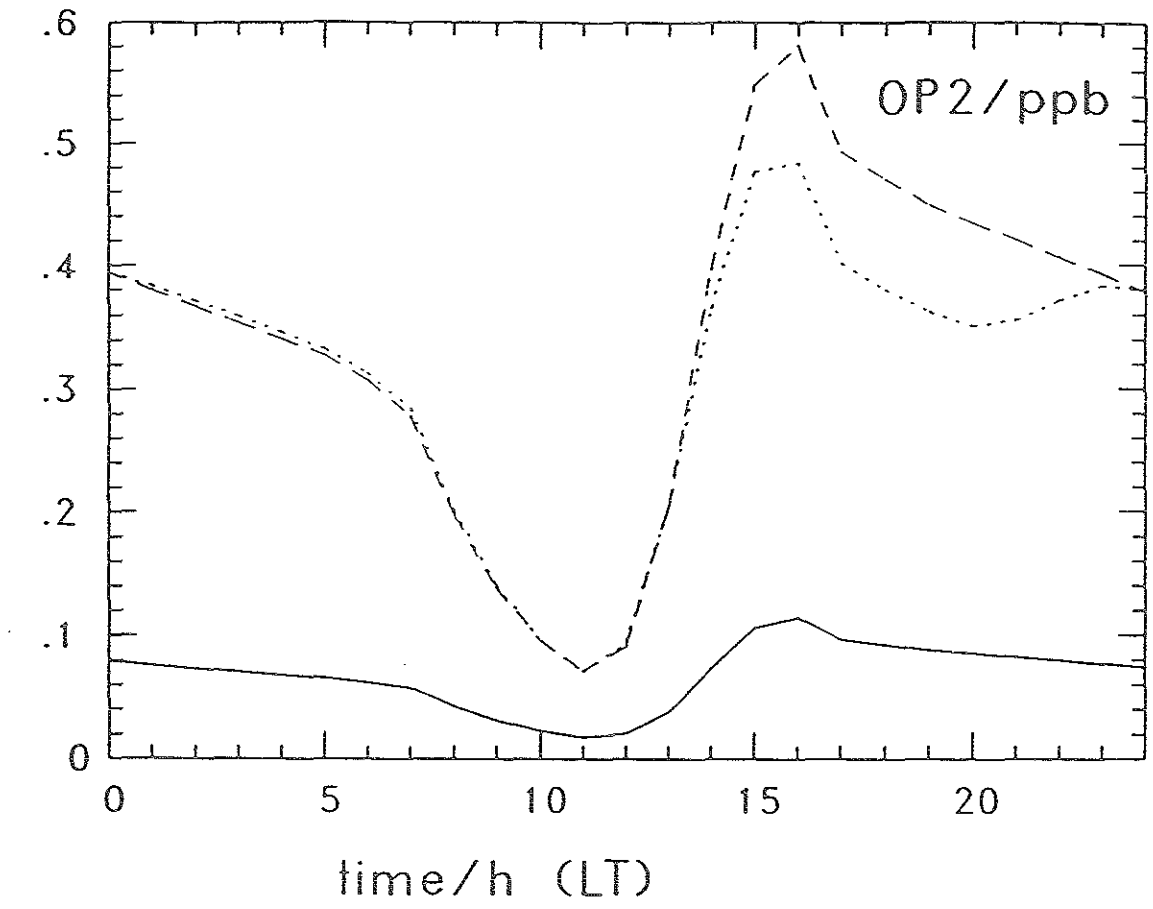
.6
.5
.4
.3
.2
.1
0
OP2/ppb
0
5
10
15
20
time/h (LT)

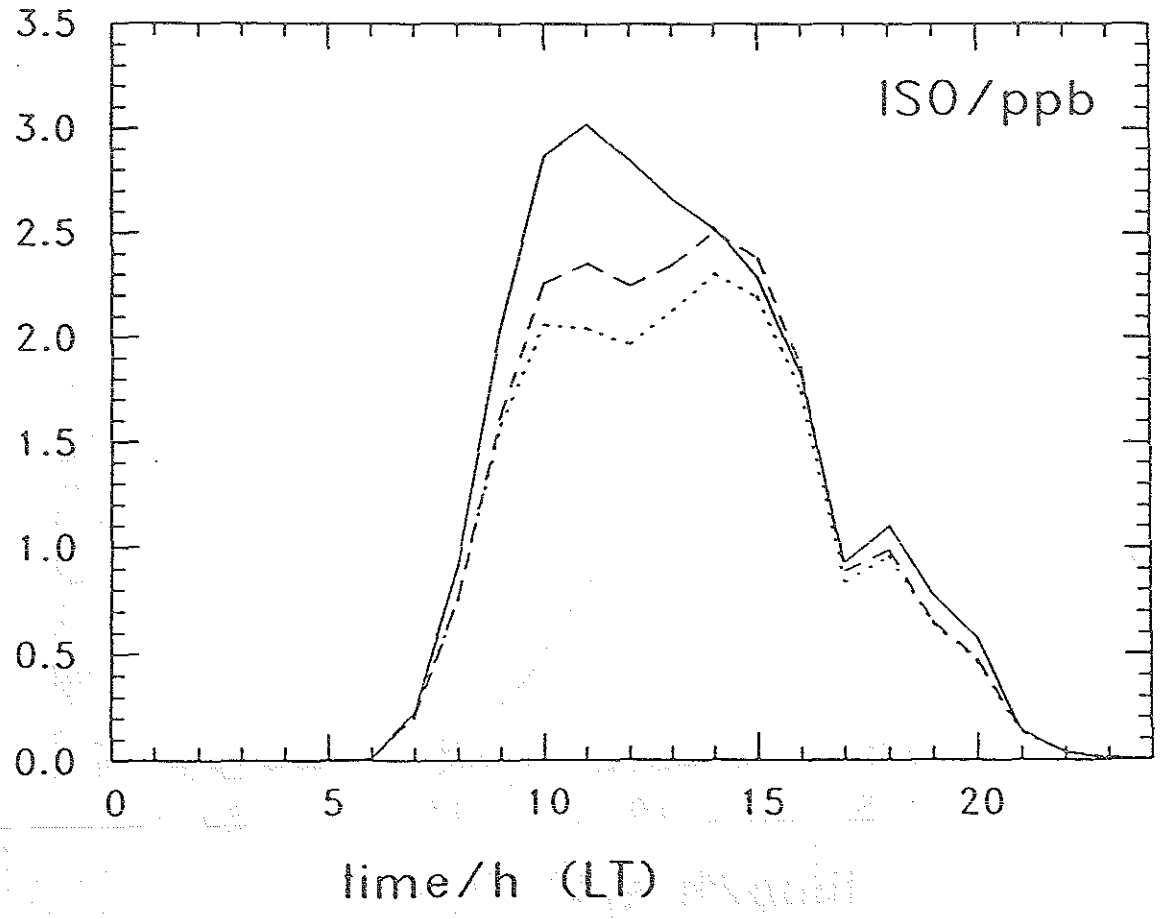
3.5
3.0
2.5
2.0
1.5
1.0
0.5
0.0
ISO/ppb
0
5
10
15
20
time/h (LT)

Fig. 3g, 3h

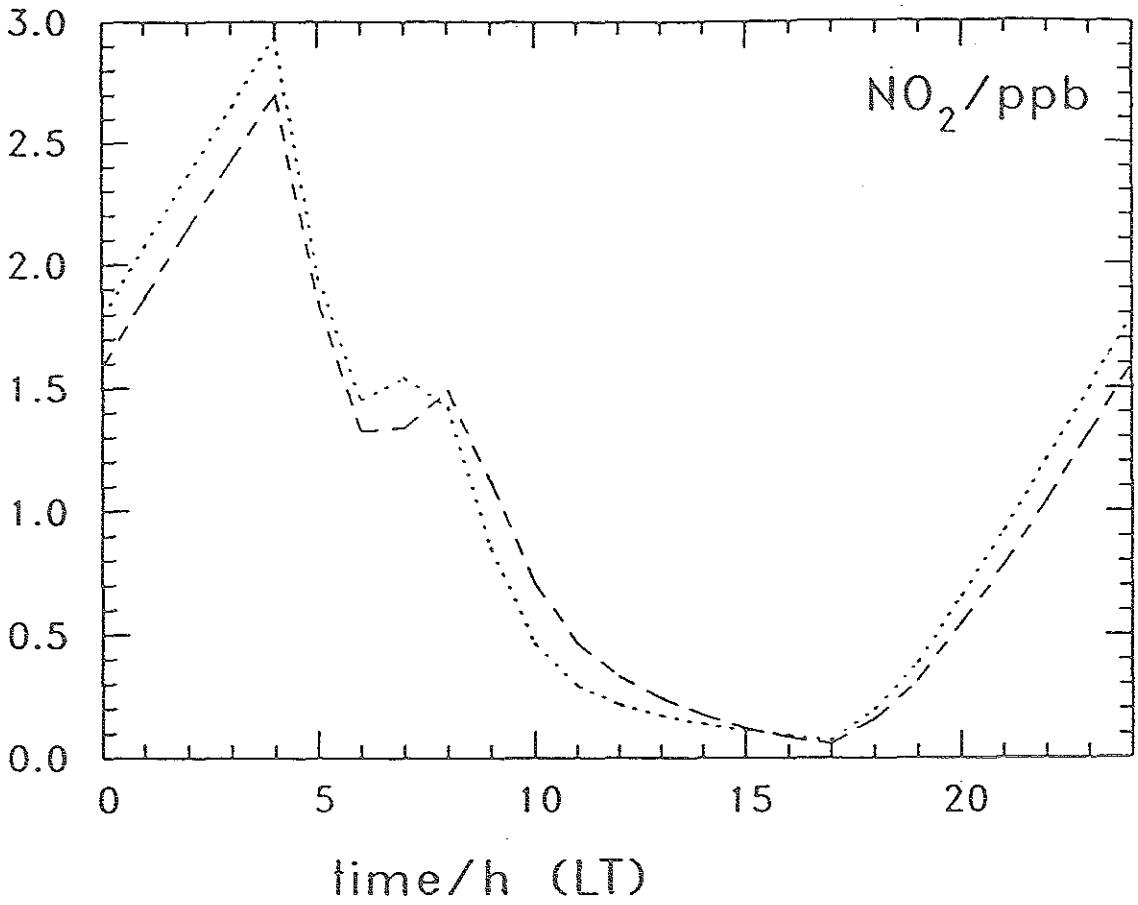
3.0
2.5
2.0
1.5
1.0
0.5
0.0
NO_2/ppb
0
5
10
15
20
time/h (LT)

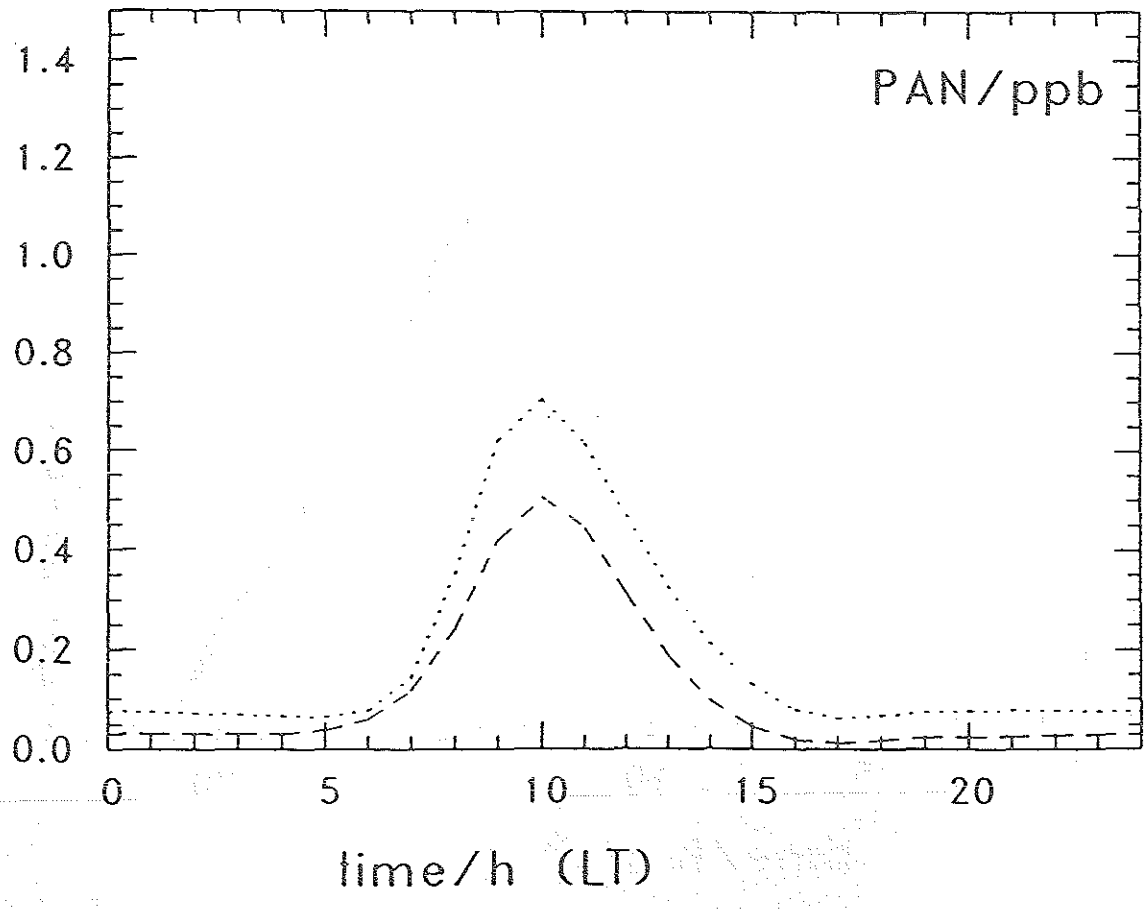
1.4
1.2
1.0
0.8
0.6
0.4
0.2
0.0
PAN/ppb
0
5
10
15
20
time/h (LT)

Fig. 4a, 4b

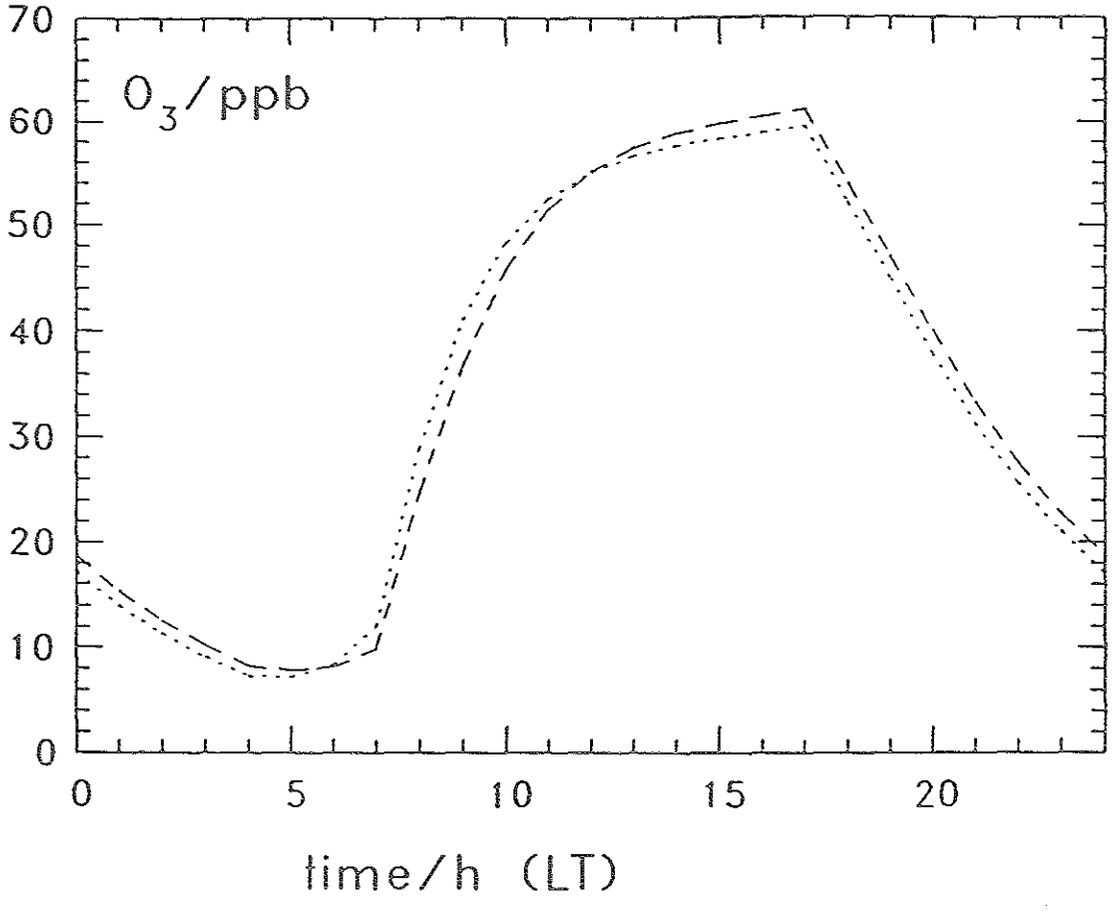
70
60
50
40
30
20
10
0
O_3/ppb
0
5
10
15
20
time/h (LT)

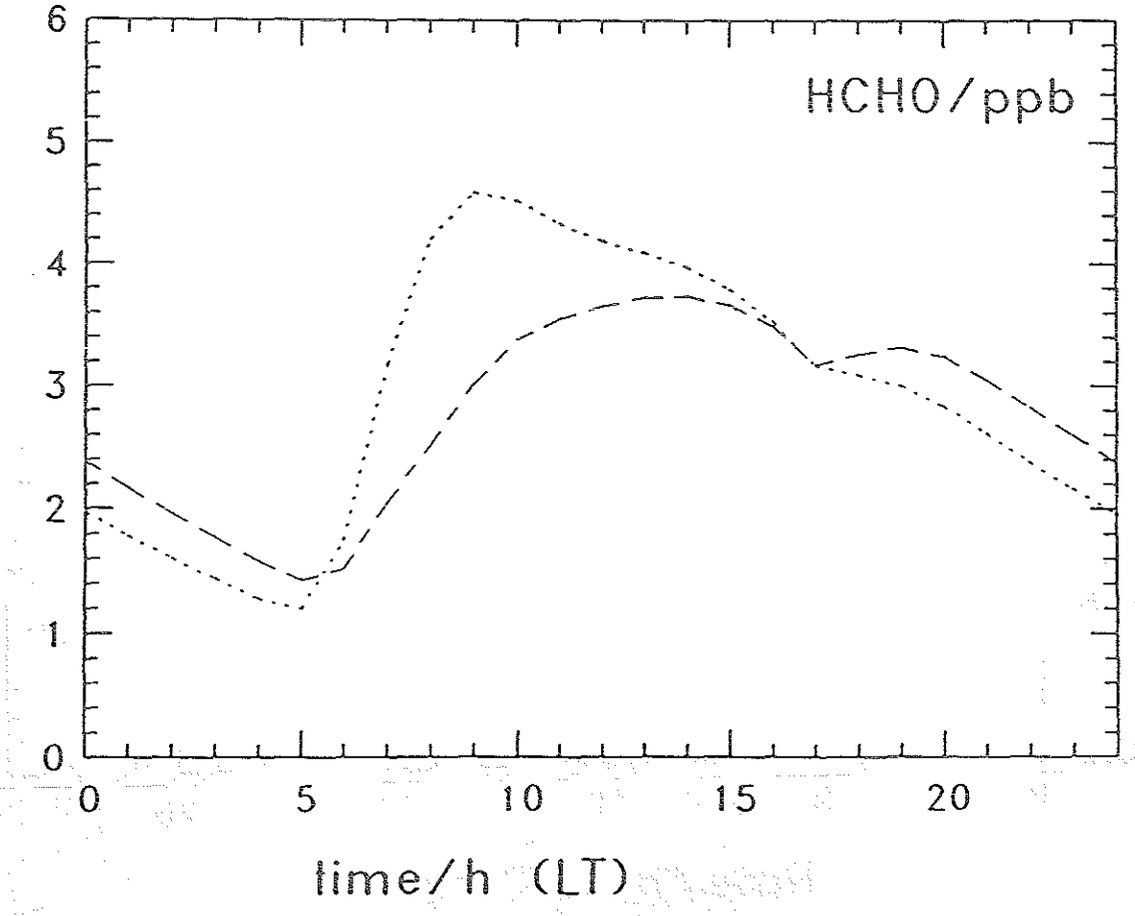
6
5
4
3
2
1
0
HCHO/ppb
0
5
10
15
20
time/h (LT)

Fig. 4c, 4d

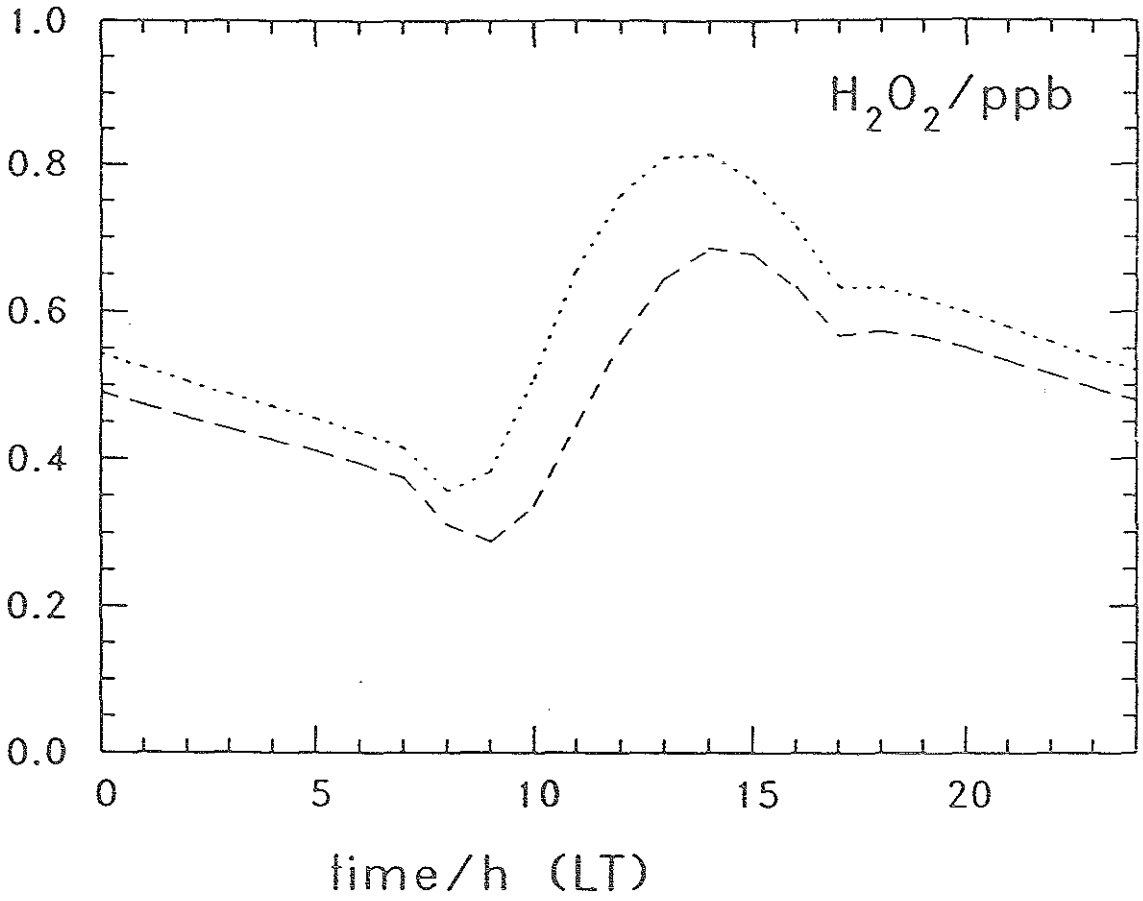
1.0
0.8
0.6
0.4
0.2
0.0
H_2O_2/ppb
0
5
10
15
20
time/h (LT)

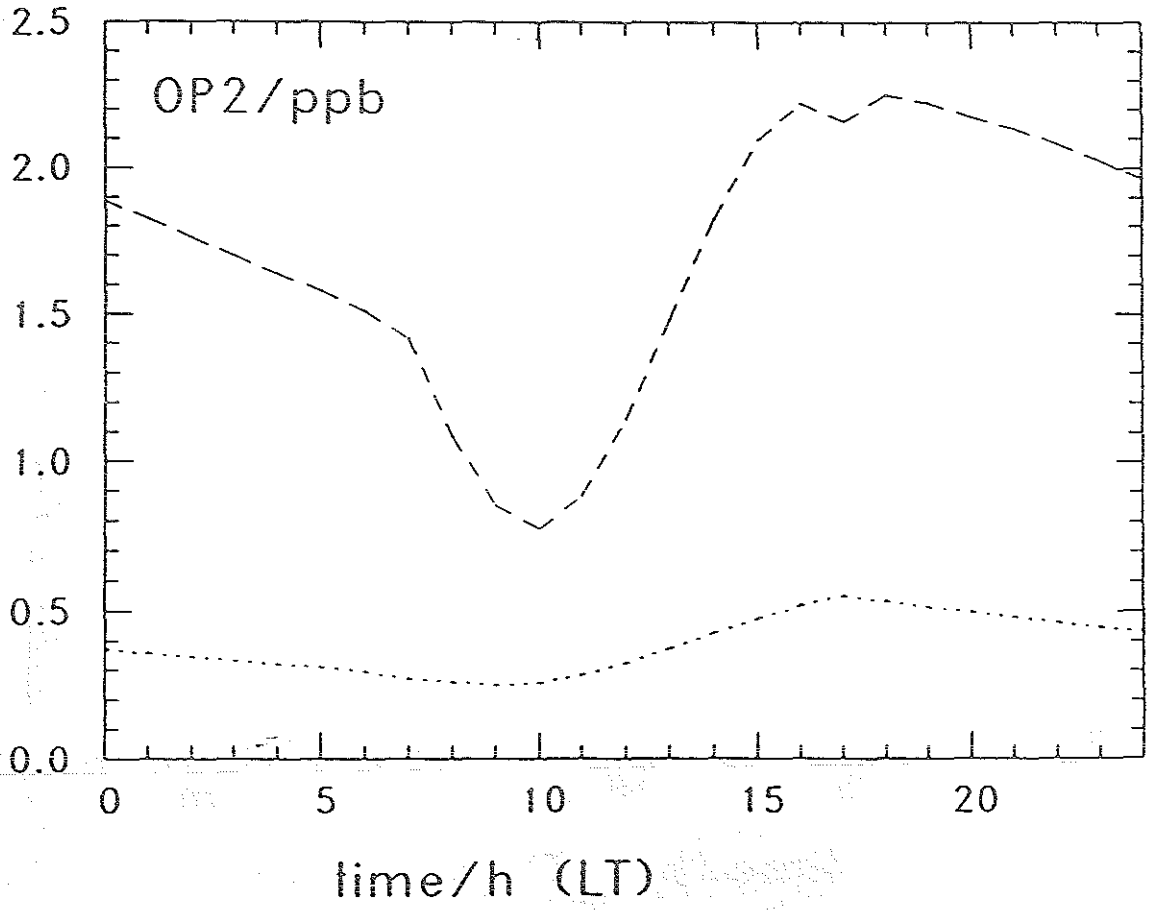
2.5
2.0
1.5
1.0
0.5
0.0
OP2/ppb
0
5
10
15
20
time/h (LT)

Fig. 4e, 4f

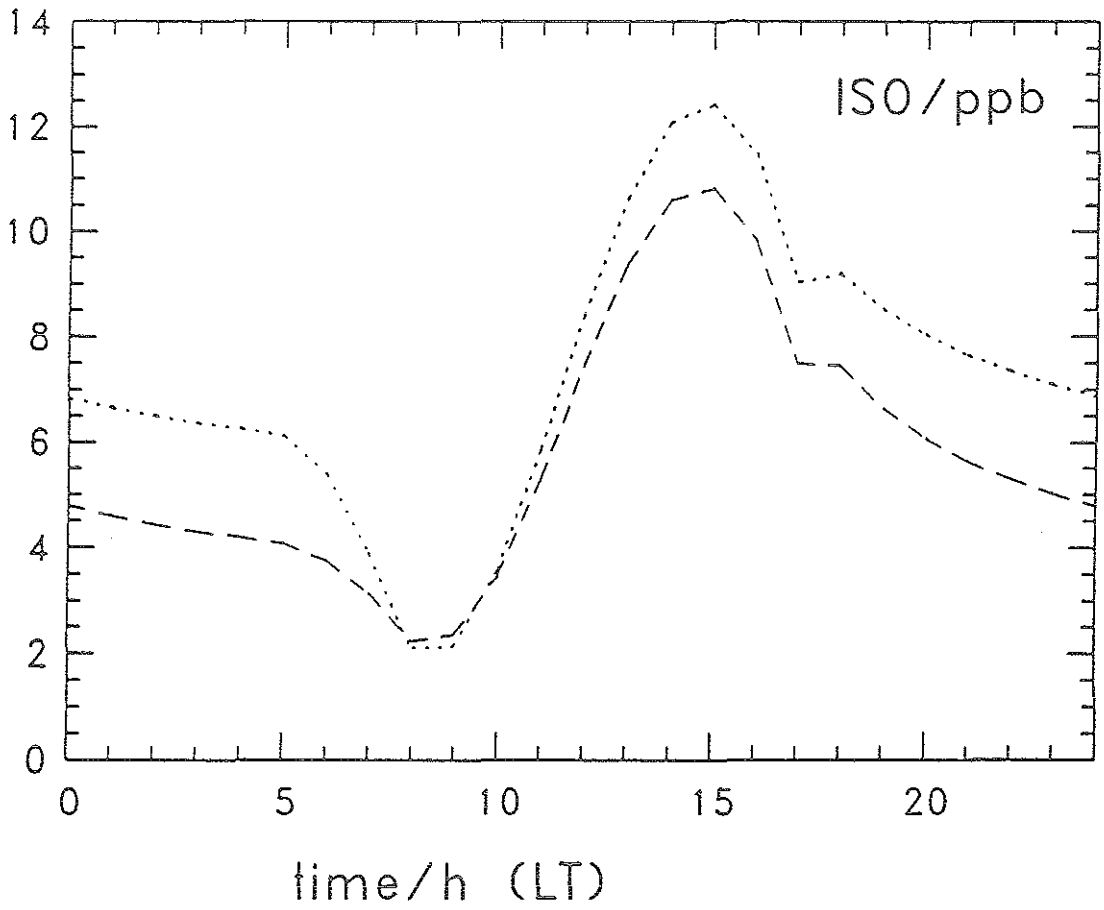

Fig. 4g

FORSCHUNGSZENTRUM JÜLICH GmbH

KFA

Jül-2938
Juli 1994
ISSN 0944-2952